Global Biogeochemical Cycles

RESEARCH ARTICLE
10.1029/2023GB007926

Special Collection:
The Arctic: An AGU Joint Special Collection

Dissolved Nitrogen Cycling in the Eastern Canadian Arctic Archipelago and Baffin Bay From Stable Isotopic Data

H. C. Westbrook[1], A. Bourbonnais[1], C. C. M. Manning[2], J.-É. Tremblay[3], M. M. M. Ahmed[4,5], B. Else[4], and J. Granger[2]

[1]School of the Earth, Ocean and Environment, University of South Carolina, Columbia, SC, USA, [2]Department of Marine Sciences, University of Connecticut, Groton, CT, USA, [3]Québec-Océan and Takuvik, Département de biologie, Université Laval, Québec, QC, Canada, [4]Department of Geography, University of Calgary, Calgary, AB, Canada, [5]Education and Research Group, Esri Canada, Calgary, AB, Canada

Abstract Climate change is expected to alter the input of nitrogen (N) sources in the Eastern Canadian Arctic Archipelago and Baffin Bay due to increased discharge from glacial meltwater and permafrost thaw. Since dissolved inorganic N is generally depleted in surface waters, dissolved organic N (DON) could represent a significant N source fueling phytoplankton activity in Arctic ecosystems. Yet, few DON data for this region exist. We measured concentrations and stable isotope ratios of DON ($\delta^{15}N$) and nitrate (NO_3^-; $\delta^{15}N$ and $\delta^{18}O$) to investigate the sources and cycling of dissolved nitrogen in regional rivers and marine samples collected in the Eastern Canadian Arctic Archipelago and Baffin Bay during the summer of 2019. The isotopic signatures of NO_3^- in rivers could be reproduced in a steady state isotopic model by invoking mixing between atmospheric NO_3^- and nitrified ammonium as well as NO_3^- assimilation by phytoplankton. DON concentrations were low in most rivers ($\leq$4.9 μmol N L^{-1}), whereas the concentrations (0.54–12 μmol N L^{-1}) and $\delta^{15}N$ of DON (−0.71–9.6‰) at the sea surface were variable among stations, suggesting dynamic cycling and/or distinctive sources. In two regions with high chlorophyll-a, DON concentrations were inversely correlated with chlorophyll-a and the $\delta^{15}N$ of DON, suggesting net DON consumption in localized phytoplankton blooms. We derived an isotope effect of 6.9‰ for DON consumption. Our data helps establish a baseline to assess future changes in the nutrient regime for this climate-sensitive region.

Plain Language Summary Primary productivity in the Arctic Ocean surface waters is limited by nitrogen supply. We investigated dissolved inorganic and organic nitrogen dynamics in the Eastern Canadian Arctic Archipelago and Baffin Bay surface ocean waters as well as adjacent rivers. We used the isotopic composition (N and O) of both dissolved organic and inorganic nitrogen (DON and DIN, respectively) to explore the sources and transformations of nitrogen. Nitrate in rivers was from both the atmosphere and nitrified ammonium. Nitrate was also consumed by phytoplankton. DON concentrations were low in rivers compared with inorganic nitrogen (i.e., nitrate). This observation contrasts with previous data collected in the Eurasian and U.S. western coastal Arctic Ocean, where rivers represent a significant source of DON to the coastal ocean. We observed variable DON concentrations and isotopic composition in the Eastern Canadian Arctic Archipelago and Baffin Bay surface ocean waters, suggesting different sources and/or a dynamic DON cycling. We additionally found evidence for DON consumption in regions of highest chlorophyll-a. These data are important to better understand how Greenland's melting ice sheet will impact nutrient delivery and primary productivity in the region.

Key Points:

- Nitrate in regional rivers was derived proximately from nitrification
- Dissolved organic nitrogen concentrations in regional rivers were low
- Dissolved organic nitrogen consumption was observed in the ECAA and Baffin Bay with the highest chlorophyll-a

Supporting Information:

Supporting Information may be found in the online version of this article.

Correspondence to:

A. Bourbonnais,
abourbonnais@seoe.sc.edu

Citation:

Westbrook, H. C., Bourbonnais, A., Manning, C. C. M., Tremblay, J.-É., Ahmed, M. M. M., Else, B., & Granger, J. (2024). Dissolved nitrogen cycling in the Eastern Canadian Arctic Archipelago and Baffin Bay from stable isotopic data. *Global Biogeochemical Cycles*, *38*, e2023GB007926. https://doi.org/10.1029/2023GB007926

Received 27 JUL 2023
Accepted 2 NOV 2024

Author Contributions:

Conceptualization: A. Bourbonnais
Data curation: A. Bourbonnais, J.-É. Tremblay, M. M. M. Ahmed, B. Else
Formal analysis: H. C. Westbrook, A. Bourbonnais, J.-É. Tremblay, M. M. M. Ahmed, B. Else
Funding acquisition: A. Bourbonnais
Investigation: H. C. Westbrook, A. Bourbonnais, C. C. M. Manning, J. Granger

1. Introduction

Climate change is rapidly altering Arctic ecosystems. As air and seawater temperatures are rising, sea ice volume is decreasing and seasonal river discharge is increasing (Bintanja & Selten, 2014; Feng et al., 2021; Wassmann et al., 2011; Wu et al., 2005). The critical roles played by the Arctic Ocean in controlling the thermohaline circulation and supporting fisheries (Link & Tol, 2009) have stimulated scientific research in the region within the past few decades. While primary productivity is expected to increase for most Arctic shelves, similar changes are not ubiquitous across the entire Arctic (Arrigo & van Dijken, 2015; Le Fouest et al., 2013; Lewis et al., 2020). Decreased nutrient delivery through physical circulation as well as increased stratification due to higher freshwater input may decrease primary productivity overall in the Canada Basin and the Eastern Canadian Arctic Archipelago (ECAA), including Baffin Bay, the Nares Strait, Lancaster Sound, and Jones Sound (Lehmann

Methodology: H. C. Westbrook, A. Bourbonnais, J.-É. Tremblay, M. M. M. Ahmed, B. Else
Project administration: A. Bourbonnais
Resources: A. Bourbonnais, C. C. M. Manning, J.-É. Tremblay, J. Granger
Supervision: A. Bourbonnais
Validation: A. Bourbonnais
Writing – original draft: H. C. Westbrook
Writing – review & editing: A. Bourbonnais, C. C. M. Manning, J.-É. Tremblay, M. M. M. Ahmed, B. Else, J. Granger

et al., 2019; McLaughlin & Carmack, 2010). Nutrients in the surface waters of the ECAA are typically low unless there are localized sources, such as rivers and inputs from glacial buoyancy-driven upwelling (Bhatia et al., 2021; Cape et al., 2019; Tank et al., 2012; Thibodeau et al., 2017). The availability of nutrients, as well as access to sunlight, are the key factors controlling primary productivity in the western Arctic basins (Tremblay et al., 2015). These factors can shift rapidly from season to season; for example, the spring freshet delivers more nutrient-rich freshwater nearshore, while increased sunlight is observed during the summer months (Holmes et al., 2012; Juranek, 2022). Nitrogen is ultimately limiting in the western Arctic (Tremblay et al., 2006; Yamamoto-Kawai et al., 2006) and thus sources and sinks of nitrogen need to be constrained to better understand the current N budget as a baseline to assess future changes.

The ECAA is fed predominantly by Pacific generated water from the Canada Basin moving eastward and exiting at Lancaster Sound. Arctic water also enters through the Nares Strait, carrying Pacific water and underlying Atlantic-origin water. In Baffin Bay, Arctic water mixes with underlying Atlantic water directly from the North Atlantic via the West Greenland current. Freshwater is also introduced into the ECAA from river and glacial melt as the coastline of the region is peppered with glaciers and has high permafrost coverage. Based on stoichiometric nutrient tracers and nitrate isotope ratios ($\delta^{15}N$), nutrients are dominantly from Pacific-derived water, albeit mixed with Atlantic-derived waters supplying about 25% of the nitrate (NO_3^-) (Lehmann et al., 2022, and references therein).

Dissolved organic nitrogen (DON) typically accounts for the largest pool of dissolved nitrogen in oligotrophic freshwater and marine surface waters (Sipler & Bronk, 2014). Although dominated by refractory species, the labile fraction of DON can be an essential source of N to primary producers, especially in N limited regions (Bronk et al., 2007; Knapp et al., 2018; Moschonas et al., 2017; Thibodeau et al., 2017). DON is composed of a highly refractory pool, a semi-labile pool, and a smaller labile pool. The timescale for utilization of DON can vary depending on lability, with refractory or semi-labile sources persisting from months to years. Labile DON can be utilized on time scales ranging from a few days to minutes in the case of amino acids (Bronk et al., 1998; Fuhrman, 1987; Sipler & Bronk, 2014). DON can be produced in situ in the oceans through mechanisms such as the viral lysing of bacteria or the loss of prey biomass during feeding by microzooplankton (Sipler & Bronk, 2014). Rivers are one of the major DON sources to the ocean due to the presence of terrestrial organic matter. As a result, DON tends to be higher in coastal areas than in the open ocean, although the utilization of DON is not limited to coastal regions (Sipler & Bronk, 2014). DON can be produced by surface plankton in productive areas and then transported out into N limited regions, fueling primary productivity (Bif et al., 2022; Knapp et al., 2018; Letscher, Hansell, Carlson, et al., 2013).

The Arctic Ocean is heavily impacted by rivers, receiving 10% of global river discharge despite accounting for only 4% of the global ocean surface (Holmes et al., 2012; Wu et al., 2005). River runoff, permafrost thaw and coastal erosion are significant sources of nutrients in Arctic coastal regions (Le Fouest et al., 2013; Tank et al., 2012; Terhaar et al., 2021; Thibodeau et al., 2017; Treat et al., 2016). Riverine input of DON is typically high in areas such as the Laptev Sea and the western Arctic, which are fed by large rivers. DON in the Lena River, which discharges into the Laptev Sea, can average between 10 and 13 μmol L^{-1} depending on the season (Sanders et al., 2022). Dissolved inorganic N delivered by rivers is immediately consumed as surface coastal Arctic waters are generally devoid of NO_3^- (Emmerton et al., 2008; Tremblay et al., 2014, 2015). The fate of riverine DON in coastal marine waters is still unclear, whether it is utilized or simply diluted through mixing with DON-depleted waters. For instance, in the Arctic surface ocean, DON concentrations are on average 4.7 μmol L^{-1}, which is less than the concentrations in major Arctic rivers, which range from 7.4 to 18.4 μmol L^{-1} (Sipler & Bronk, 2014). Tank et al. (2012) suggested that riverine NO_3^- and DON in the coastal Laptev Sea region contribute to overall Arctic Ocean primary productivity, albeit for a relatively small fraction (<10% each). They suggest that riverine DON in the Arctic is slowly remineralized, allowing for nutrient transport from the coastal areas into ocean basins. Thibodeau et al. (2017) found that DON concentrations discharged from the Lena River in the Eurasian Arctic were up to 6 times higher than riverine NO_3^- concentrations and that DON was rapidly consumed nearshore, with over 50% of it disappearing before reaching the shelf. However, Dittmar et al. (2001) concluded that DON input from Siberian rivers did not substantially support primary productivity as it was largely recalcitrant. With riverine discharge increasing since around the 1960s (Peterson et al., 2002; Wu et al., 2005), the extent to which rivers influence the delivery of bioavailable DON in Arctic coastal waters needs to be further investigated.

While previous studies have largely focused on the inputs of nutrient from large rivers in past decades (e.g., Tank et al., 2012; Thibodeau et al., 2017), deliveries of NO_3^- and dissolved organic nitrogen (DON) by small rivers and

glacially fed rivers (e.g., proglacial rivers), and their impacts on coastal oceanic primary productivity in the ECAA and Baffin Bay have not been thoroughly explored. Inputs of NO_3^- to surface waters have been shown to occur by upwelling induced by rising submarine glacial melt discharge in proximity to the Greenland Ice Sheet and Jones Sound (Bhatia et al., 2021; Cape et al., 2019) and glacial melt (Beaton et al., 2017). However, the input of exogenous DON to the surface ocean from glacial melt has not been considered thus far. Upwelling regions generally see elevated DON concentrations following the increase in biological activity due to NO_3^- input from below (Sipler & Bronk, 2014). Since many rivers are of glacial origin in the ECAA and Baffin Bay, both glacial and terrestrial riverine end members must be constrained to identify the sources of DON in this rapidly changing region.

The naturally occurring stable N and O isotope ratios of the dissolved N species can be exploited to identify N sources and transformations in environmental samples. The nitrogen $^{15}N/^{14}N$ isotope ratios are reported in delta notation (δ) and units of per mil (‰), where the $^{15}N/^{14}N$ and $^{18}O/^{16}O$ references are atmospheric N_2 (i.e., air) for N and Vienna Standard Mean Ocean Water (VSMOW) for O.

$$\delta^{15}N = \left[\left(\left({}^{15}N \,/\, {}^{14}N_{sample}\right)/\left({}^{15}N \,/\, {}^{14}N_{air}\right)\right) - 1\right] \times 1000$$

$$\delta^{18}O = \left[\left(\left({}^{18}O \,/\, {}^{16}O_{sample}\right)/\left({}^{18}O \,/\, {}^{16}O_{VSMOW}\right)\right) - 1\right] \times 1000$$

The $\delta^{15}N{-}NO_3^-$ and DON are influenced originally by the $\delta^{15}N$ of its source(s) and secondarily by the fractionation imposed during phytoplankton uptake and DON decomposition (see Knapp et al., 2005). The $\delta^{15}N{-}NO_3^-$ and DON can thus be diagnostic of dominant sources of new N in a system. The DON produced by N_2-fixing organisms as well as newly nitrified NO_3^- from this source are expected to reflect the low $\delta^{15}N$ of newly fixed ammonium (NH_4^+; −2 to 0‰) (Carpenter et al., 1997; Knapp et al., 2018; Minagawa & Wada, 1986). N from atmospheric deposition is associated with a similarly low $\delta^{15}N$ (Altieri et al., 2016 and references therein). Conversely, the $\delta^{15}N{-}DON$ released by phytoplankton is generally more elevated, reflecting the $\delta^{15}N$ of the incident inorganic N substrates. The $\delta^{15}N$ of nitrate varies regionally, posting a global ocean average of ∼5‰, but the $\delta^{15}N$ of Pacific waters of western Arctic basins is distinctly higher at 8‰ due to benthic coupled nitrification-denitrification processes (Granger et al., 2018). DON and NO_3^- produced through newly regenerated N, typically NH_4^+, will often have a lower $\delta^{15}N$ compared to ambient substate pools as lighter isotopes are preferentially excreted (Fawcett et al., 2011).

In turn the $\delta^{18}O$ of NO_3^- is distinct among N sources and also sensitive to NO_3^- production and consumption terms. The $\delta^{18}O$ of NO_3^- in atmospheric deposition is exceptionally high (e.g., Hastings et al., 2003). Nitrate produced by the nitrification of ammonium empirically converges on $\delta^{18}O$ of water (Buchwald et al., 2012; Casciotti et al., 2010). Assimilatory and dissimilatory NO_3^- consumption results in a parallel increase of both $\delta^{18}O$ and $\delta^{15}N$ in a 1:1 ratio (Granger et al., 2004, 2008) in proportion to nitrate consumed. This relationship can be used to determine the influence of processes other than assimilation on the NO_3^- pool.

The goals of this study are to determine, using an isotopic approach, (a) the dominant sources of NO_3^- and DON in the ECAA and Baffin Bay and (b) the transformations affecting these pools. This study focuses on the Nares Strait, Jones Sound, Lancaster Sound, and Baffin Bay, whose coastal regions are more extensively bordered by glaciers compared to other Arctic regions and experience a large amount of glacial runoff (Rogalla et al., 2023). Nutrient input from the numerous small glacially fed rivers in this region is not as well characterized as that from the large terrestrial rivers in other Arctic regions such as the Laptev Sea and the western Arctic (Letscher, Hansell, Kadko, & Bates, 2013; Thibodeau et al., 2017). This region of the Arctic also experiences high continuous permafrost coverage, the degradation of which could be a source of labile nitrogen in local rivers (Francis et al., 2023; Frey et al., 2007). Eastern Baffin Bay is also a highly productive area important for fisheries in Greenland. Determining the sources of nutrient inputs to coastal waters is essential to predict the effect of climate change on primary productivity in these economically important regions. Furthermore, Baffin Bay (via the Davis Strait) accounts for roughly a third of all freshwater input from the Arctic to the North Atlantic, including both liquid freshwater and sea ice (Haine et al., 2015). Shifts in the transport and cycling of nitrogen within the ECAA due to changes in glacial coverage, permafrost melt, or other climate change effects could translate to broader impacts outside the Arctic.

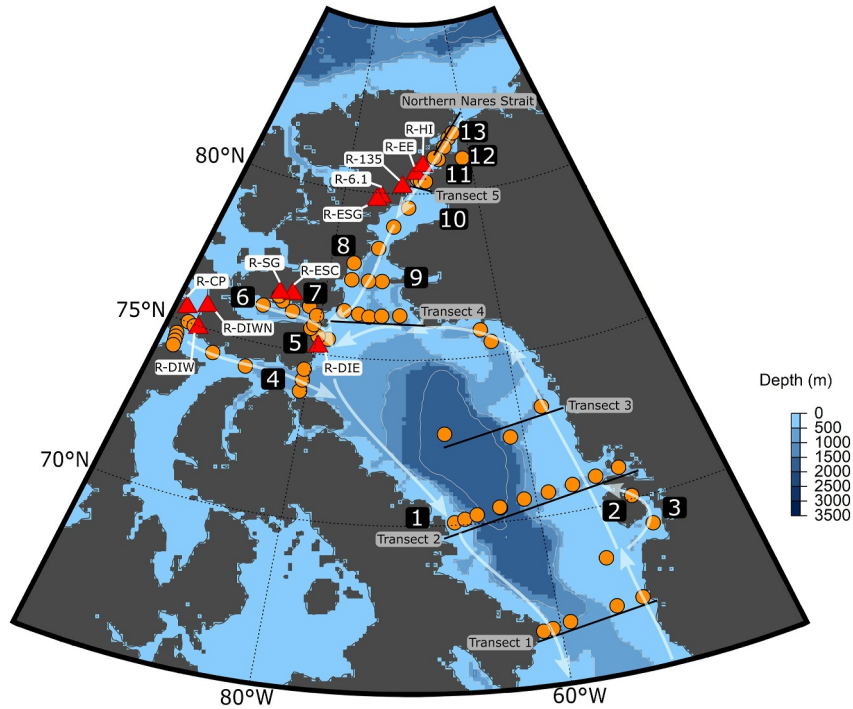

Figure 1. Map of the sampling locations. CTD casts are marked with orange circles. Red triangles represent river locations, which are also labeled by name. Transects 1–5, and the Northern Nares Strait are labeled with solid black lines. The directions of surface currents are shown by the white arrows. Important regions and features are as follows: 1: Clyde River, 2: Disko Island, 3: Jakobshavn Glacier, 4: Lancaster Sound, 5: Devon Island, 6: Jones Sound, 7: Manson Icefield, 8: Talbot Inlet, 9: Smith Sound, 10: Kane Basin, 11: Kennedy Channel, 12: Petermann Glacier, 13: Hall Basin. 9–13 are all considered part of the Nares Strait.

2. Materials and Methods

2.1. Regional Setting and Sample Collection

Samples were collected during Legs 2a and 2b of the ArcticNet expedition aboard the Canadian Coast Guard Ship (CCGS) *Amundsen* from July 5th to August 15th of 2019. The expedition took place in the ECAA including Baffin Bay, the Nares Strait, Lancaster Sound, and Jones Sound (Figure 1). In this region, prevailing currents flow southward through Nares Strait and into Kane Basin, Smith Sound, and finally Baffin Bay. In northwestern Baffin Bay, currents flow eastward from Lancaster Sound into Baffin Bay. At the surface, these water masses are Pacific-derived and circulate in the Canadian and Makarov Basins before entering the ECAA through the Nares Strait and Lancaster Sound, respectively. In Baffin Bay, Atlantic water enters along the southwestern coast of Greenland and travels north until it converges with water flowing south from the Smith Sound and circulates southwards on the eastern side of Baffin Island (Lehmann et al., 2019, 2022; Tang et al., 2004). Atlantic water from the Eurasian Basin of the Arctic Ocean can be found at depth in Baffin Bay (Alkire et al., 2010). Ice cover in this region varies by season and along an east-west gradient, with the lowest coverage in the summer and ice persisting much longer on the western side of Baffin Bay in spring (Tang et al., 2004). Some sea ice in Baffin Bay is formed locally, while some is formed in the Nares Strait and transported south. Ice formed in other channels is typically blocked by landfast ice and does not enter Baffin Bay (Tang et al., 2004).

Samples for the analysis of DON concentration and isotopic composition were collected using 12 L Niskin bottles at depths of 100 and 80 m, and then upwards to the surface in 10 m intervals. Samples at 100 and 80 m were collected in 15 mL centrifuge tubes, and samples taken above 80 m were collected in 60 mL high-density polyethylene (HDPE) plastic bottles. All centrifuge tubes and bottles were acid-washed and rinsed three times with sample water prior to collection. All samples were frozen with a headspace to allow water expansion upon freezing until analysis. Samples taken during Leg 2b were also filtered with GF/F filters before freezing. Leg 2a samples were filtered prior to analysis with Supor™ 0.45 micron polyethersulfone filters. A comparison was

performed on the effect of the different filters on [DON] and $\delta^{15}N-DON$ and no significant difference was observed. Riverine samples were collected from the surface waters of 11 rivers, filtered with GF/F filters, and frozen. Due to methodological limitations, not all samples collected were analyzed for [DON] and $\delta^{15}N$ of DON; this is expanded upon in Section 2.2. Water samples were also collected for $\delta^{18}O$ of H_2O analysis; samples were collected without bubbles in 2 mL glass vials and stored at 4°C.

2.2. Concentration and Isotopic Analysis of DON, NO_3^-, and $\delta^{18}O$ of H_2O

$[NO_3^-]$, $[NO_2^-]$ and $[PO_4^{3-}]$ were measured at sea using a Bran and Luebbe Autoanalyzer III. Working standards were prepared at each station and checked against reference standard material (KANSO CRM, lots CI and CG to cover the range of Atlantic- and Pacific-derived waters in the region). Ammonium concentration in riverine samples was measured using a SEAL AQ300 Discrete Analyzer following the U.S. Environmental Protection Agency (EPA) salicylate method EPA-148-D.

The concentration and $\delta^{15}N$ of DON were measured as in Knapp et al. (2005). Briefly, total dissolved nitrogen (TDN) was oxidized to NO_3^- using recrystallized persulfate followed by measurement on a NO_x analyzer by chemiluminescent detection (Braman & Hendrix, 1989). The $\delta^{15}N$ of TDN (oxidized to NO_3^-) was then analyzed using the denitrifier method (Sigman et al., 2001; Weigand et al., 2016). As there is currently no efficient means to remove DIN, the combined concentration and isotopic composition of NO_3^-, NO_2^-, and NH_4^+ (if present) must be analyzed to calculate the $\delta^{15}N$ of DON by isotopic mass balance. $[NO_3^- + NO_2^-]$ was thus also measured by chemiluminescence prior to persulfate oxidation and the $\delta^{15}N-NO_3^-$ was determined using the denitrifier method (Casciotti et al., 2002; Sigman et al., 2001; Weigand et al., 2016). Only samples in which DON represents over 50% of TDN were analyzed for isotopic composition. This is because as the ratio of DON to DIN decreases, the error associated with the $\delta^{15}N$ of DON calculated by isotopic mass balance increases.

To prepare samples for isotopic analysis of DON, 1 mL of freshly prepared persulfate oxidizing reagent (POR) was added to 6 mL of sample in 12 mL threaded test tubes with Teflon-lined phenolic screw caps (Corning 99447-161). These samples were then autoclaved for 1 hr and analyzed for [TDN]. The POR blank was typically <0.4 μmol $L^{-1}$and [TDN] was corrected for blank contribution. The international standards USGS40, USGS64, and USGS65 and an internal standard of 6-aminocaproic acid (5 μmol L^{-1}) were analyzed within each run to verify oxidation efficiency and that no fractionation occurred during the persulfate oxidation step. The average percent yield of standard concentrations was >95%, and the standard deviation from known isotopic composition was ±0.4‰.

Prior to isotopic analysis, the pH of the autoclaved samples, standards, and blanks was adjusted to 3–4 with 6N HCl. Neutralized samples were injected into 2 mL of *Pseudomonas chlororaphis* suspended in media. When analyzing NO_3^- alone, *Pseudomonas aureofaciens* was instead used to measure the $\delta^{18}O$ of NO_3^-. In the samples in which NO_2^- accumulated, NO_2^- was removed using sulfamic acid, as in Granger and Sigman (2009). The target sample size was 20 nmol. The product N_2O was purified and analyzed using a continuous flow isotope ratio mass spectrometer (Elementar Americas PrecisION) equipped with a custom on-line gas extraction and purge-trap system and PAL autosampler. Samples were standardized using a two-point correction with the international standards IAEA-NO-3 ($\delta^{15}N = 4.7‰$ vs. air) and USGS34 ($\delta^{15}N = -1.8‰$ vs. air). The $\delta^{15}N$ of DON was determined by isotopic mass balance taking into consideration the concentration and $\delta^{15}N$ of the POR blank as well as sample NO_3^- and TDN. The average standard deviation for duplicate $\delta^{15}N$-DON analysis was generally lower than ±0.5‰. Error propagation was determined using a Monte Carlo method, as in Knapp et al. (2018).

The $\delta^{18}O$ of H_2O was measured using an integrated off-axis cavity absorption spectrometer (Los Gatos Research, LGR, Triple Liquid Water Isotope Analyzer, model 912-0032) at the University of Calgary as described in Ahmed et al. (2020). Chlorophyll-a was measured using High Performance Liquid Chromatography (HPLC) at the University of British Columbia as described in Burt et al. (2018). $\delta^{18}O$ of H_2O and salinity were used to calculate fractions of freshwater and sea ice melt, as described in Supporting Information S1. Plots of surface data and cross-sections were generated with the Ocean Data View software (Schlitzer, 2021).

2.3. Model for Riverine NO_3^- Cycling

A simple steady-state isotopic model was used to apportion the sources and sinks of NO_3^- in ECAA and Baffin Bay rivers based on previously established understandings of riverine nitrogen cycling and the isotopic

composition of nitrogen and oxygen sources in Arctic riverine ecosystems. We then compared NO_3^- values to our model to explore potential influences on NO_3^- in rivers. This model included two sources of NO_3^- supplied to rivers: (a) NO_3^- from the nitrification of NH_4^+, sourced from permafrost, atmospheric NH_4^+, or in-river mineralization (e.g., Alves et al., 2013; Fouché et al., 2020; Wagner et al., 2002) and (b) uncycled NO_3^- from atmospheric deposition (e.g., Hastings et al., 2004).

We assumed that complete nitrification of NH_4^+ results in NO_3^- with a $\delta^{15}N$ of ∼1.2‰ akin to atmospheric and permafrost end members (range: −6–10‰ (Ansari et al., 2013; Arendt et al., 2016; Clark et al., 2020; Heikoop et al., 2015; Louiseize et al., 2014; Wynn et al., 2007)). The $\delta^{18}O$ produced during the nitrification of NH_4^+ was estimated to be ∼−14.2‰ (range: −8.9 to −19.5‰), assuming that at least 2/3 of the O atoms are derived from water during nitrification (Boshers et al., 2019; Casciotti et al., 2010; Heikoop et al., 2015). For this estimation, we assume the $\delta^{18}O$ of water ranged from −12‰ to −22‰ (Arendt et al., 2016; Wynn et al., 2007) and that the $\delta^{18}O$ of dissolved oxygen ranged from 23.5‰ to 24.2‰ based on the $\delta^{18}O$ of air (Kiddon et al., 1993; Wang & Veizer, 2000; Wynn et al., 2007 and references therein). We assumed isotope effects of the $\delta^{18}O$ of NO_3^- and exchange with H_2O during bacterial nitrification, as in Casciotti et al. (2010) and Buchwald et al. (2012). We also assumed that NH_4^+ was completely oxidized to NO_3^- in rivers, as NH_4^+ was absent or very low in all our samples, with the highest concentration being 0.56 μmol L^{-1} at R-ESC. We assumed that atmospheric deposition added NO_3^- with a $\delta^{15}N$ of −3.5‰ and a $\delta^{18}O$ of 72.1‰ (Ansari et al., 2013; Hastings et al., 2004; Heikoop et al., 2015; Louiseize et al., 2014).

We assumed a kinetic N isotope effect (ε) of 6.0‰ for NO_3^- assimilation (Rafter & Sigman, 2016) and a corresponding $^{18}\varepsilon$:$^{15}\varepsilon$ of 1:1 (Granger et al., 2004). The isotope effect is defined as $^{15}\varepsilon\,(\text{in}\,‰) = [(({}^{14}k/{}^{15}k) - 1) \times 1000]$, where ^{14}k and ^{15}k are the rate coefficients of the reactions for the light and heavy isotopes, respectively. We excluded denitrification, the canonical conversion of NO_3^- to the nitrogen gases N_2O and N_2 under anaerobic conditions, due to the high O_2 concentrations in the rivers (Dalsgaard et al., 2014). We considered two main scenarios for the extent of N recycling and its impact on primary production within the rivers: (a) 50% recycled production, and (b) 25% recycled production. These parameters were chosen as plausible scenarios based on estimates of nutrient recycling in the Arctic (Tank et al., 2012; Whalen & Cornwell, 1985). More details about the model are included in Supporting Information S1.

We used this model to reproduce the deviation from the $^{18}\varepsilon$:$^{15}\varepsilon$ ratio of ∼1 observed for pure NO_3^- assimilation (Granger et al., 2004) of our riverine samples. We refer to this deviation as the Δ(15,18), which is the difference between NO_3^- $\delta^{15}N$ and $\delta^{18}O$ (Rafter et al., 2013).

2.4. Isotope Effect of DON Consumption

In areas where chlorophyll-a was the highest, we estimated the $^{15}\varepsilon$ of surface mixed layer DON consumption using a closed system Rayleigh distillation model ($\delta^{15}N$ of DON vs. ln[DON]) as in Knapp et al. (2018). A low [DON] concomitant with elevated $\delta^{15}N$ indicates consumption, as kinetic isotope fractionation during consumption increases the $\delta^{15}N$ of the residual DON pool.

3. Results

3.1. Physical Characteristics of the ECAA and Baffin Bay

Near shore waters were influenced by freshwater input from rivers and/or glacial meltwater, as evidenced by fresher surface waters with distinctly low $\delta^{18}O$ H_2O values (−6.05 to −0.54‰). Freshwater influx was evident throughout the study region, particularly near Talbot Inlet, the Petermann Glacier, the Jakobshavn Glacier, in Lancaster Sound, and near the riverine stations R-SG and R-ESC in Jones Sound (Figure S1A in Supporting Information S1).

Within the Nares Strait, Jones Sound, and Lancaster Sound, water at depth was predominantly Pacific derived. Along Eastern Baffin Bay, the input of Atlantic waters was observed at depth, due to the West Greenland current, which carries North Atlantic water into Baffin Bay. Finally, in Western Baffin Bay, there was an initial increase in Pacific derived water at depth and then a decrease as the waters mixed with Atlantic derived water (Figure S2 in Supporting Information S1). This was consistent with previous observations of water masses in the area (Lehmann et al., 2022, and references therein).

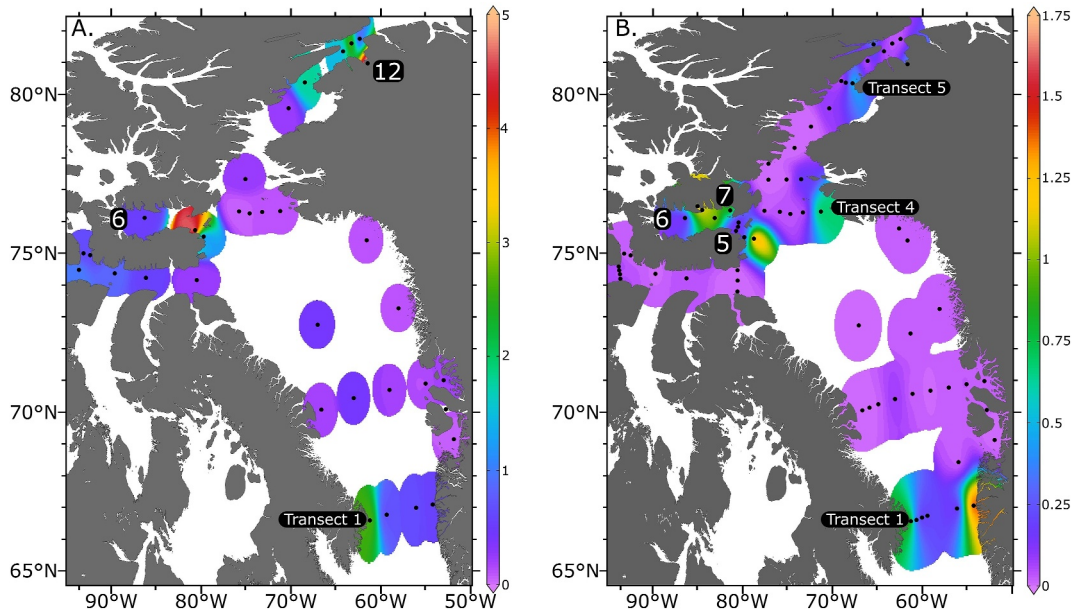

Figure 2. (a) Surface chlorophyll-a (μg L^{-1}). (b) [NO_3^-] (μmol L^{-1}) distribution in surface waters of the study area. 1—Clyde River, 3—Jakobshavn Glacier, 5—Devon Island, 6—Jones Sound, 8—Talbot Inlet, 12—Petermann Glacier.

Many of the rivers sampled in this study were glacially fed, particularly those on Ellesmere Island, such as R-ESG and R-6.1. Others were not located near glaciers, for example, R-DIW and R-DIW-N on western Devon Island, and R-CP on Cornwallis. Rivers ranged from 0.5 to 3 m deep and ∼1 to ∼30 m wide. $\delta^{18}O$ of H_2O in rivers ranged from −18.4 to −28.4‰ (Brown et al., 2022). Satellite imagery of the river sampling locations is provided in Figures S3–S6 in Supporting Information S1.

3.2. Chlorophyll-a

Chlorophyll-a concentrations at the surface (4 m) were low throughout the study region (typically <2 μg L^{-1}) except in the northern Nares Strait, where a particularly large bloom near Petermann Glacier was observed, as well as in Jones Sound, and the western side of Transect 1 (Figure 2a).

3.3. Nitrate Concentration and Isotopic Composition in the ECAA and Baffin Bay

Nitrate concentration was near zero in all surface waters, except in the Jones Sound, as well as the eastern and western ends of the Davis Strait (Transect 1 in Figures 1 and 2b). At Transect 1, the $\delta^{15}N{-}NO_3^-$ was lower in the east (6.5‰), and higher in the west (9.8‰), where a higher chlorophyll-a concentration was also observed (Figure 2a). $\delta^{18}O$ of NO_3^- across this transect was similar in the east (3.3‰) and west (3.4‰). At the mouth of the Jones Sound, a $\delta^{15}N$ and $\delta^{18}O$ of NO_3^- of 14‰ and 50‰ were observed. Nitrate was generally completely consumed in the mixed layer (upper 10 m) within the study area and increased with depth to up to ∼15 μmol N L^{-1} at 100 m depth (Figure 3).

Nitrate concentration and isotopic composition of river samples are provided in Table 1. The concentration of NO_3^- among riverine samples covered a broad range, from 0.44 to 47 μmol L^{-1} (Table 1). NO_2^- concentrations were <0.2 μmol L^{-1} in all samples, both riverine and marine, expect for R-6.1, which had 1.4 μmol L^{-1} NO_2^-. High variability was observed even in rivers adjacent to one another, such as R-6.1 and R-ESG. The isotopic composition of NO_3^- was highly variable between rivers, indicating variability in NO_3^- sources and/or transformations. R-SG had the lowest $\delta^{15}N{-}NO_3^-$ (0.71‰) and a [NO_3^-] of 2.7 μmol L^{-1}. R-ESG had the highest $\delta^{15}N{-}NO_3^-$ (10.3‰) and a [NO_3^-] of 0.44 μmol N L^{-1}. The adjacent river R-6.1, which was about 20–30 m wide, had a similarly elevated $\delta^{15}N{-}NO_3^-$ of 10‰ but much higher [NO_3^-] of 11 μmol L^{-1}. In contrast, R-ESG was a river running through a crevasse adjacent to Eugenie Glacier and was only ∼1 m wide. R-ESG and R-6.1 were drastically different with respect to their $\delta^{18}O$ of NO_3^-, which was −2.7‰ in R-6.1 and 49‰ in R-ESG.

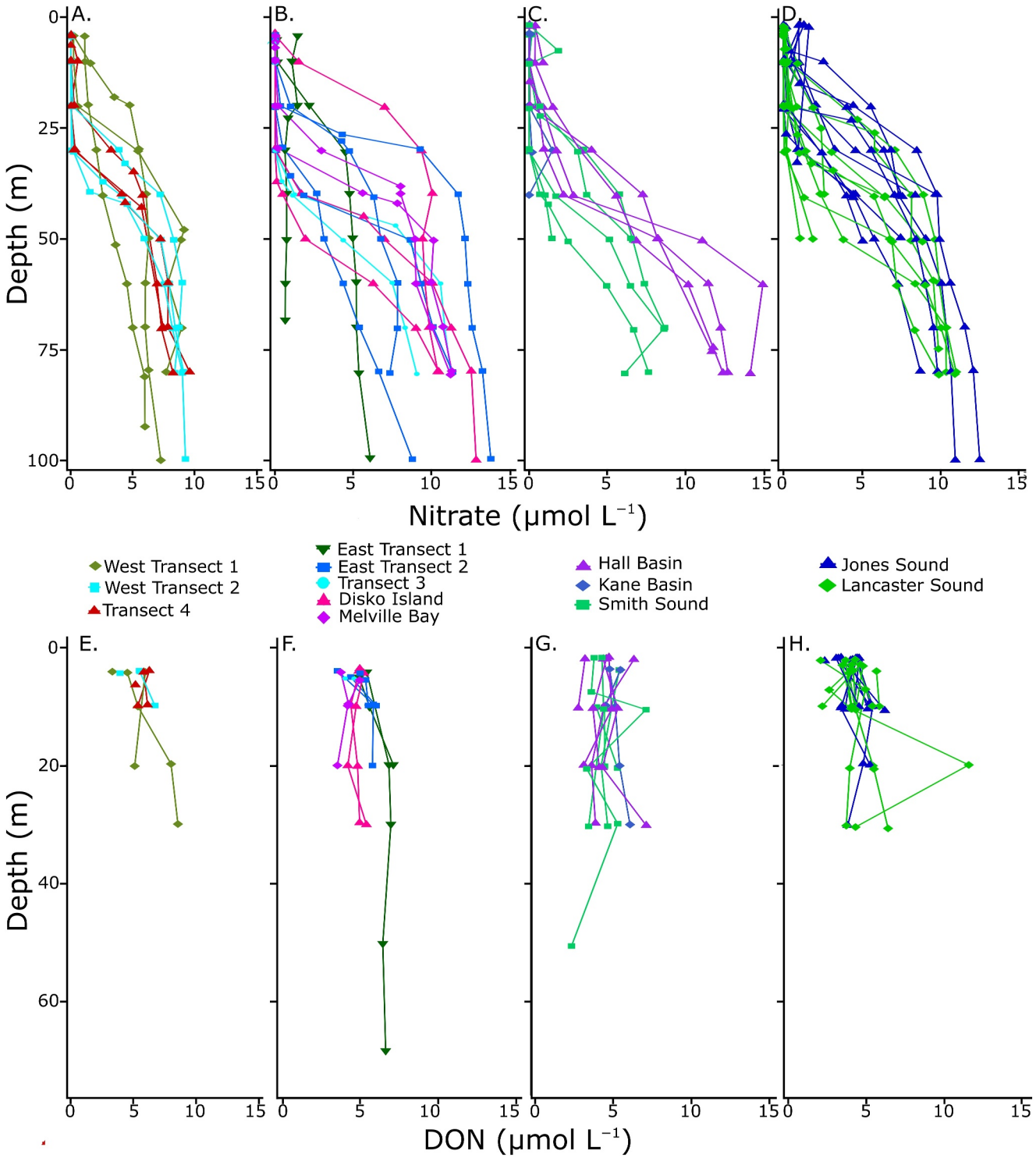

Figure 3. NO_3^- (top) and DON (bottom) concentration depth profiles for (a) and (e) Western Baffin Bay; (b) and (f) Eastern Baffin Bay; (c) and (g) Nares Strait; and (d) and (h) Jones and Lancaster Sounds.

Table 1
Concentration and $\delta^{15}N$ and $\delta^{18}O$ of NO_3^- and DON, As Well As Δ(15,18) of NO_3^- (Calculated as in Rafter et al., 2013) and Notable Features of River Samples

Station Unit	$[NO_3^-]$ μmol L^{-1}	$\delta^{15}N-NO_3^-$ ‰	$\delta^{18}O-NO_3^-$ ‰	Δ(15,18) ‰	[DON] μmol L^{-1}	$\delta^{15}N-DON$ ‰	Notable features and location
Glacial							
R-DIE	1.30	3.40	18	−14	0.54	NA	Drains Devon Ice Cap, rocks and sand; Devon Island
R-ESC	3.30	2.60	−6.3	8.9	1.80	NA	Compact sand, rocks; Ellesmere Island
R-SG	2.70	0.71	−1.4	2.1	3.10	5.8	Multiple glaciers, rocks and sand; Ellesmere Island
R-6.1	11.00	10.00	−2.7	13	0.00	NA	Adjacent to glacial moraine, silt, mud and clay; Ellesmere Island
R-ESG	0.44	10.00	49	−38	4.90	7.2	Within glacier, silt, clay, pebbles; Ellesmere Island
R-135	3.50	6.60	7.3	−0.68	0.16	NA	Rocks, sand and silt; Ellesmere Island
R-EE	2.70	4.80	10	−5.4	1.50	NA	Rocks, some sand and silt; Ellesmere Island
R-HI	4.70	5.30	−0.80	6.1	1.40	NA	Rocks, sand, mud; Ellesmere Island
Terrestrial							
R-CP	4.10	2.90	−7.5	10	2.20	NA	Downstream of lake, icy at edge, medium and large flat rocks, possibly shale; Cornwallis Island
R-DIW	20.00	4.40	−9.3	14	1.60	NA	Medium and large flat rocks and sandstone; Devon Island
R-DIW-N	47.00	4.80	−9.6	14	0.99	NA	Greenery at mouth, medium rocks and mud; Devon Island

Note. "R" denotes the rivers sampled. Rivers were named based on proximity to geographic features or CTD stations: Devon Island East (R-DIE), Eastern Sydkap Icecap (R-ESC), Sydkap Glacier (R-SG), Station 6.1 (R-6.1), Eugenie's Sister Glacier (R-ESG), Station 135 (R-135), Ellesmere Island East (R-EE), Hans Island (R-HI), Copland Point (R-CP), Devon Island West (R-DIW), and Devon Island West North (R-DIW-N). Rivers are divided by their dominant landscape.

There was no correlation between the $\delta^{15}N-NO_3^-$ and $\ln([NO_3^-])$ in rivers ($P = 0.72$, $R^2 = 0.05$), but $\delta^{18}O$ of NO_3^- was strongly negatively correlated with $\ln([NO_3^-])$ ($P = 0.002$, $R^2 = 0.63$), as shown in Figure 4.

High variation was also observed between R-ESC and R-SG, both of which are west of Grise Fjord. R-SG was around 5 m wide and ~0.5 m deep, while R-ESC was roughly 20 m wide and between 1 and 2 m deep. R-ESC was more inland than R-SG. R-SG and R-ESC had similar NO_3^- concentrations, but the $\delta^{15}N-NO_3^-$ was almost 2‰ higher at R-ESC than R-SG. Furthermore, the $\delta^{18}O$ of NO_3^- at R-ESC was nearly 4.5 times lower than that at R-SG. Conversely, two other stations in similar areas, R-DIW and R-DIW-N, both located on the west side of Devon Island had significantly different NO_3^- concentrations (20 and 47 μmol L^{-1}, respectively), but similar isotopic signatures (e.g., 4.4‰ and 4.8‰ for $\delta^{15}N$ of NO_3^-, respectively).

We considered that the isotopic composition of riverine NO_3^- was derived from two end-member sources, namely NO_3^- produced proximately by nitrification and uncycled atmospheric NO_3^-. However, the NO_3^- isotopic composition of our samples did not fall along the mixing line for the two end members. The isotope values were explained by also invoking the partial assimilation of NO_3^- and associated isotopic enrichment of residual NO_3^- (Figure 5). This indicates that atmospheric depositions, assimilation and nitrification contributed, to some extent, to the $\delta^{15}N$ and $\delta^{18}O$ of NO_3^- signatures of the river samples.

We used a steady-state isotopic model to confirm that these three processes (nitrification, atmospheric depositions and NO_3^- assimilation) could produce a deviation from the $^{18}\varepsilon:^{15}$ ε ratio of ~1 observed for pure NO_3^- assimilation (Granger et al., 2004) for our riverine samples. We define the deviation from the $^{8}\varepsilon:^{15}$ ε ratio of ~1 as the difference between NO_3^- $\delta^{15}N$ and $\delta^{18}O$, referred to as Δ(15,18) (Rafter et al., 2013). Assuming that 25%–50% of the dissolved nitrogen was recycled within the rivers, we were able to reproduce the full range of observed Δ(15,18) (Figure 6).

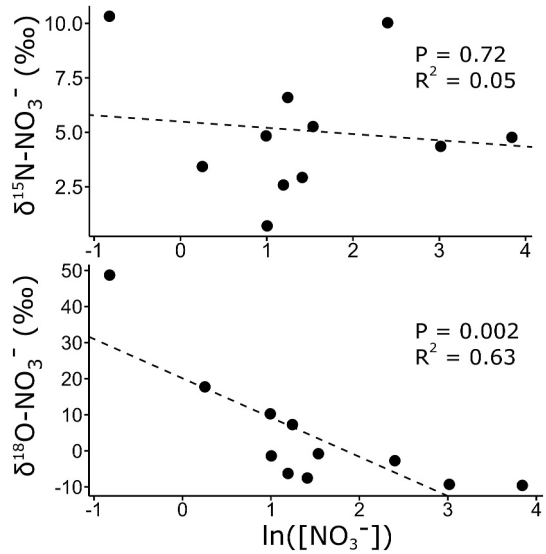

Figure 4. The $\delta^{15}N$ (top) and $\delta^{18}O$ (bottom) of NO_3^- against $\ln([NO_3^-])$ in all rivers sampled. Pearson's correlation coefficient and *P* are also included.

3.4. DON Distribution and $\delta^{15}N$ in the ECAA and Baffin Bay

The surface distribution of [DON] and $\delta^{15}N$ of DON are shown in Figure 7. DON concentrations were highly variable but had similar values between regions, ranging from 3.2 to about 6.0 μmol L^{-1} in Baffin Bay and the Nares Strait. Lancaster Sound and Jones Sound had lower DON concentrations, ranging from 2.1 to 5.7 μmol L^{-1}.

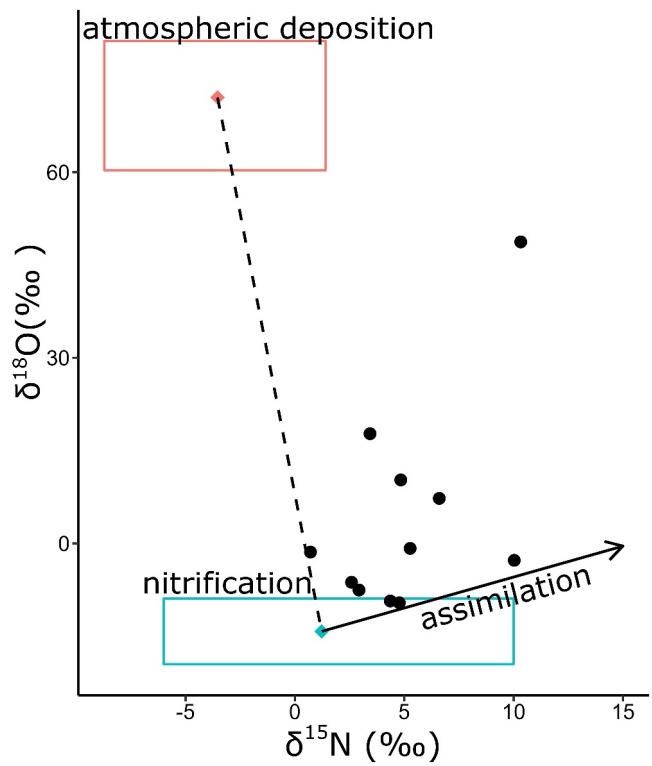

Figure 5. $\delta^{18}O–NO_3^-$ versus $\delta^{15}N–NO_3^-$ for riverine samples, with mixing between nitrification of NH_4^+ (blue box) and atmospheric deposition (pink box) marked by the dashed line. The ε^{18}: ε^{15} of assimilation (~1) is noted with the solid black arrow.

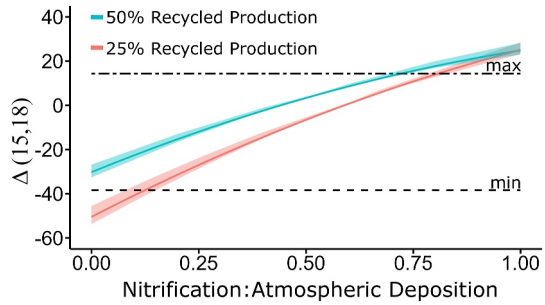

Figure 6. Results from simple box model simulations evaluating the capacity of different sources of NO_3^- in glacial rivers of the ECAA to generate $\delta^{15}N$ and $\delta^{18}O$ and $\Delta(15,18)$ signatures. The ratio of nitrified NH_4^+ to atmospheric deposition is on the *x* axis, and $\Delta(15–18)$ on the *y*-axis. The blue line represents 50% recycled production, and the pink line represents 25% recycled production. The shaded colors represent model outputs when using the outer ranges of the end members. The black dashed lines represent the minimum and maximum $\Delta(15,18)$ observed in the riverine samples.

In the mixed layer (upper 10 m) of the water column, [DON] increased with salinity (Figure 8). [DON] in riverine samples were moderate-to-low (0–4.9 μmol L^{-1}), even when [NO_3^-] was high. Due to the presence of NO_3^-, the $\delta^{15}N$ of DON could only be measured at R-SG and R-ESG (5.8 and 7.2‰ respectively).

However, no significant relationship between [DON] and the fraction of freshwater input was observed in Jones Sound, where the highest freshwater fraction was calculated (Figure 2a). [DON] did not fall directly along the pure mixing line at most stations, suggesting surface ocean DON production and consumption processes (Figure 8). The relationship between DON concentration and $\delta^{15}N$ with depth was variable and often only characterized within the upper 40 m because NO_3^- concentrations below 40 m depth were often too high to allow calculating the $\delta^{15}N$ of DON from isotopic mass balance. Depth profiles of [DON] are depicted in the bottom panel of Figure 3. Concentration and $\delta^{15}N$ of DON increased with depth in Transects 1 and 2 of Lancaster Sound, and in some areas near Disko Island. The depth relationship between [DON] and $\delta^{15}N$ was more variable at some of the more southernmost stations, ranging from an increase in [DON] and a slight decrease in $\delta^{15}N$, a slight increase in both $\delta^{15}N$ and [DON], or no change in isotopic composition.

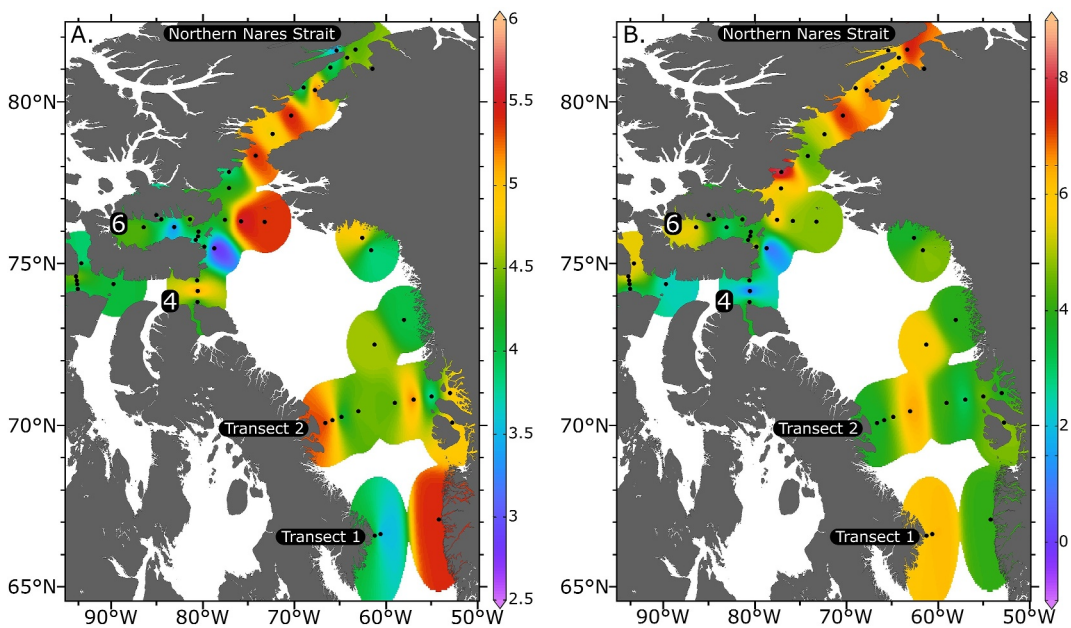

Figure 7. (a) [DON] (μmol L^{-1}) and (b) $\delta^{15}N$ of DON (‰) in the surface water. Transects 1, 2, and Northern Nares Strait are denoted with black boxes. Lancaster (4) and Jones (6) Sounds are also labeled.

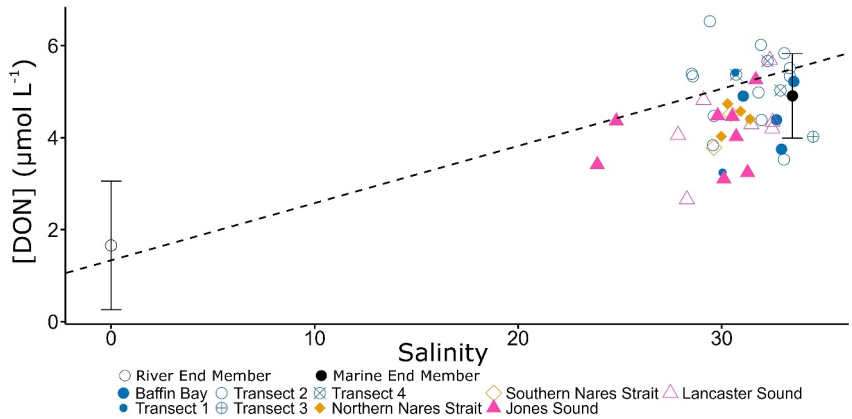

Figure 8. [DON] (µmol L^{-1}) in the mixed layer (upper 10 m) of the water column versus salinity. Blue dots represent samples located within Baffin Bay, orange diamonds represent samples in Nares Strait, and pink triangles represent samples located in sounds to the east of Baffin Bay. Riverine (hollow) and marine (solid) end members are marked with black dots with solid lines representing the standard deviation for end member estimates. The dashed line represents mixing between the two end members.

In two areas where highest chlorophyll-a concentrations were measured, the Northern Nares Strait and Western Transect 1, chlorophyll-a and DON concentrations in the upper 10 m were inversely correlated (Pearson $R^2 = 0.75$, p-value = 0.04; Spearman $\rho = -1$; Figure 9) and ln([DON]) and δ^{15}N-DON were also inversely correlated (Pearson $R^2 = 0.54$, p-value = 0.10; Spearman $\rho = -1$ and p-value = 0.02; Figure 10). These trends were not observed in Jones Sound, where relatively high chlorophyll-a concentrations were also observed. Furthermore, no relationships were observed between the freshwater fraction and [DON] or freshwater fraction and δ^{15}N of DON in the Northern Nares Strait and Western Transect 1, precluding a significant source of low [DON] and elevated δ^{15}N−DON from rivers at these locations.

4. Discussion

4.1. Nitrogen Cycling in ECAA Rivers

Baffin Bay, through the Davis Strait, accounts for one third of all Arctic riverine discharge into the North Atlantic; therefore, major shifts in river discharges are expected to significantly impact nutrient cycling in the region (Haine et al., 2015). River discharges from Arctic watersheds are steadily increasing in response to changes in the North Atlantic Oscillation and global mean surface air temperature (McClelland et al., 2016; Peterson et al., 2002; Rood et al., 2017). In fact, small watersheds feeding minor rivers have been warming at faster rates than large ones (such as the Lena and Mackenzie river watersheds). They also cover areas that are at a high risk of permafrost degradation and contain large amounts of soil-bound carbon (Speetjens et al., 2023). Arctic rivers can transport massive quantities of dissolved and particulate inorganic and organic nitrogen, sustaining primary productivity in

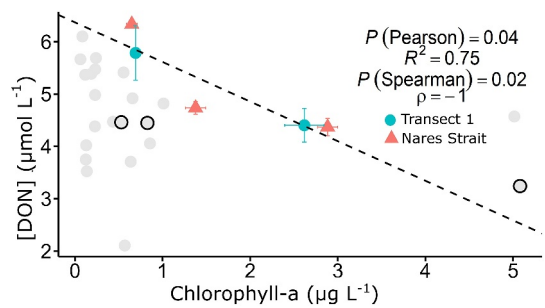

Figure 9. [DON] (µmol L^{-1}) in the northern Nares Strait (north of 80°N) (comprising Hall Basin and Kennedy Channel) and western Transect 1, against chlorophyll-a concentration (µg L^{-1}). Data are from the upper 10 m. The Pearson and Spearman's rank correlation coefficients and p-values (P) are shown. Data from all other stations are shown with light gray dots, with Jones Sound outlined in black.

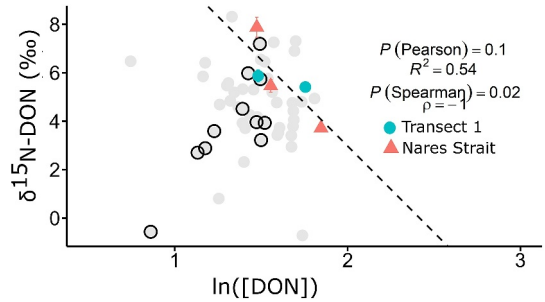

Figure 10. Ln(DON) versus $\delta^{15}N$ of DON in the northern Nares Strait (north of 80°N) and western Transect 1. Data are from the upper 10 m of the water column. The Pearson and Spearman's rank correlation coefficients and *p*-values (P) are shown. Data from all other stations are shown with light gray dots, with Jones Sound outlined in black.

coastal waters (Letscher, Hansell, Kadko, & Bates, 2013; McClelland et al., 2016; Thibodeau et al., 2017). Conversely, increased river discharge and coastal erosion can lead to unfavorable nearshore light conditions, which could negatively impact primary productivity (Terhaar et al., 2021). Our data suggest that the nutrient composition of the small but numerous rivers in the ECAA is not comparable to major terrestrial rivers in other Arctic regions.

The concentration and isotopic composition of riverine NO_3^- in this study were highly spatially distinctive, indicating variable contributions of end-member sources as well as production and consumption terms. We considered two main sources of NO_3^- in rivers: atmospheric deposition or the proximate nitrification of NH_4^+ from either permafrost or atmospheric deposition (and internal recycling). Some rivers with low [NO_3^-] had particularly high $\delta^{18}O$, up to 48‰, suggesting a significant fraction of uncycled atmospheric NO_3^-. The $\delta^{18}O$ of NO_3^- from atmospheric deposition in the summer reflects the $\delta^{18}O$ of the O sources, which are ozone (O_3) and hydroxyl radicals (OH). O_3 has a higher $\delta^{18}O$ (90–122‰; Johnston & Thiemens, 1997; Krankowsky et al., 1995), while OH usually has $\delta^{18}O < 0$ (Hastings et al., 2004). NO_3^- receives two O atoms from O_3, and one from OH, significantly increasing the $\delta^{18}O$ of NO_3^- from atmospheric deposition (65.2–79.6‰; Hastings et al., 2004).

Other rivers had a low $\delta^{18}O$ of NO_3^- (7 out of 11 rivers with $\delta^{18}O$ of $NO_3^- < 0$‰), which portends the nitrification of exogenous and recycled NH_4^+. During nitrification, most of the O atoms originate from water, hence the $\delta^{18}O$ of newly nitrified NO_3^- approaches the O isotopic signature of its H_2O source (Boshers et al., 2019). Since freshwater in high latitude systems has a lower $\delta^{18}O$ of H_2O (~−22‰; Arendt et al., 2016; Louiseize et al., 2014), the low $\delta^{18}O$ of NO_3^- observed in some ECAA river waters could indicate a significant input from nitrification. Nitrification within the rivers is supported by the observed negative correlation between $\delta^{18}O$–NO_3^- and ln[NO_3^-] (Figure 4).

The NO_3^- isotopic signatures (both $\delta^{15}N$ and $\delta^{18}O$) suggested that mixing between atmospheric NO_3^- and nitrified NH_4^+ alone could not account for the observed $\delta^{15}N$ and $\delta^{18}O$. To determine the contribution of these end members, we used a steady-state isotopic model described in Section 2.3 and Supporting Information S1, and were able to reproduce the range of observed $\delta^{15}N$, $\delta^{18}O$ as well as $\Delta(15,18)$ in riverine samples (Figure 6). Including NO_3^- assimilation helped explain the observed dual NO_3^- isotopic values (solid arrow in Figure 5). This requirement for NO_3^- removal by assimilation is corroborated by previous studies, which have observed the uptake of NO_3^- by phytoplankton in Arctic rivers (Beaton et al., 2017; Snyder & Bowden, 2014). Our isotopic model also suggests that the majority of our data appear to be more influenced by the input of microbially derived (nitrified) NO_3^- rather than uncycled atmospheric NO_3^-. The ratio of nitrification to atmospheric deposition was between 0.12 and 0.82, with the ratio of most samples over 0.5 (Figure 6). This indicates that nitrification is putatively an important process to provide bioavailable N to Arctic rivers. This influence is likely seasonally dependent. Rivers in this study were sampled after the early melt season (early June to mid−July), during which remineralization takes over as the dominant source of NO_3^- as opposed to atmospheric NO_3^- deposition (Louiseize et al., 2014).

Two major potential sources of nitrified NH_4^+ could be permafrost or atmospheric deposition. Some Canadian Arctic permafrost is known to contain a large quantity of NH_4^+ (Fouché et al., 2020) and contact with permafrost can influence the chemical composition of rivers (Frey & McClelland, 2009; Frey et al., 2007;

Heikoop et al., 2015; Vonk et al., 2015). However, rivers in direct contact with organic matter sources such as permafrost and debris are typically DON-rich (Fouché et al., 2020; Frey & McClelland, 2009; Frey et al., 2007; Wadham et al., 2016), and most of the rivers in this study were DON-depleted (Table 1). NH_4^+ can also be found in atmospheric deposition in similar proportions to atmospheric NO_3^- (Clark et al., 2020; Fouché et al., 2020). This could indicate that the nitrified NO_3^- in these rivers was sourced from the atmospheric deposition of NH_4^+.

This is not to rule out any influence of permafrost derived NO_3^- on these rivers. While we did not see the characteristic high [DON] observed in rivers with increased permafrost coverage, we were unable to analyze δ^{15}N-DON due to analytical limitations in all but two of our riverine samples (R-SG and R-ESG) as [DON] was less than 50% of the TDN pool. As a result, we do not have much insight into DON cycling within these rivers. Future studies should better constrain the isotopic composition (δ^{15}N) and lability of permafrost DON as well as soil conditions, which can affect nitrogen cycling. Frey et al. (2007), for example, suggest that organic nitrogen in the permafrost of Alaskan watersheds was more easily remineralized compared to West Siberian watersheds, as the Siberian watersheds have high water saturation, which can limit remineralization of DON and facilitate denitrification. Improvements to the analytical methods for measuring stable isotopes of DON (e.g., the capability to remove DIN prior to DON analysis) could elucidate the contribution of permafrost in delivering DON to glacially fed rivers.

Prior studies have observed low δ^{15}N-DON in rivers and streams, at around −4 to 2‰ (Thibodeau et al., 2017; Ye et al., 2018). These values have been attributed to N sources from atmospheric deposition, aquatic and/or terrestrial N_2 fixation, or plant litter decomposition. Assuming that DON sources in these rivers would have similar δ^{15}N to this range, the δ^{15}N-DON in R-SG and R-ESG was slightly elevated (5.8‰ and 7.2‰, respectively). This may indicate kinetic isotope fractionation during consumption or a source of recalcitrant DON with a particularly high δ^{15}N. DON consumption will preferentially utilize the lighter isotopes, elevating the δ^{15}N-DON of the remaining pool (Bourbonnais et al., 2009; Knapp et al., 2005, 2018).

R-ESG also had a very distinct δ^{18}O-NO_3^- signature of atmospheric NO_3^-, and a Δ(15,18) that could indicate NO_3^- assimilation based on our model results (Figure 6). Coupled low [NO_3^-] and relatively higher [DON] (Table 1) could indicate the consumption of atmospherically derived NO_3^- producing DON. R-ESG's low [NO_3^-] (0.44 μmol L^{-1}) and high δ^{18}O–NO_3^- (49‰) directly contrasts with those of the adjacent river R-6.1 (11 μmol $L^{-1}$and −2.7‰). We attribute this extreme variability to different landscape features associated with these rivers. R-ESG was running directly through a glacier, while R-6.1 was next to a glacial moraine containing significant terrestrial material. Therefore, R-ESG was likely in more direct contact with the glacial end member and thus might have a relatively higher atmospherically derived NO_3^- fraction. R-6.1, on the other hand, has a Δ (15,18) that could indicate a predominantly nitrified source of nitrate. R-6.1 was devoid of DON, which could also indicate limited interaction with the permafrost at this location. We posit that the sources of nitrogen in these rivers greatly vary depending on watershed characteristics and microbial metabolisms as suggested by Kaiser et al. (2017), even within small spatial scales.

DON concentrations previously reported for glacial rivers are greatly variable depending on the characteristics of the glacier it is fed by and the interactions of the melt water with the surrounding features. Studies on the Leverett Glacier, a land terminating glacier on the Greenland Ice Sheet adjacent to eastern Transect 1, reported a range from 5.1 to 14.0 μmol L^{-1} for DON in the surface ice, while DON in basal ice and summer ice melt was on average about 3.0 and 12.0 μmol L^{-1}, respectively (Holland et al., 2019; Wadham et al., 2016). Higher DON values were attributed to the presence of debris or microbial production of DON. However, other studies reported near zero DON concentration in supraglacial streams, cryoconite melt water, snow, and short ice cores (Holland et al., 2019; Telling et al., 2012; Wadham et al., 2016). Runoff from the Leverett Glacier, which feeds into the Watson River, also had a relatively low average DON concentration of 1.7 μmol L^{-1}, with a maximum of 6.3 μmol L^{-1} (Wadham et al., 2016). Thus, the low [DON] seen in river samples in this study could be characteristic of glacial melt that has not significantly mixed with high DON basal ice or debris.

The type of soil in this study region also likely influences the input of DON in small Arctic rivers. The sediment in most of the rivers sampled mostly consisted of sand and rocks, even those that were not adjacent to glaciers. The fact that the terrestrial rivers sampled in Western Lancaster Sound (R-CP, R-DIW, and R-DIW-N) all had relatively low [DON] (0.99–2.2 μmol L^{-1}) compared to large terrestrial rivers in other regions indicates that the sediments at these locations are likely low in organic matter. High dissolved organic carbon

(DOC) concentrations have been observed in Arctic regions with fine-grained watersheds, whereas DOC tended to be lower when the watershed consisted of coarser grains and shallow bedrock (O'Donnell et al., 2016). However, this region also contains high continuous permafrost coverage, and as permafrost degrades, it is expected to significantly release organic matter into the surrounding water bodies (Francis et al., 2023; Frey et al., 2007). When considering the nutrient forcings in this region, it is thus important to consider the influence of both glacially fed rivers, and small terrestrial rivers with low organic matter concentrations.

Particulate nitrogen (PN) can also significantly impact the N pool in riverine and marine ecosystems. In larger Arctic rivers, the relationship between PN and DON can vary greatly. One study, for instance, found that the annual PN yield in the Yenisey is much lower than that of DON, but in the Kolyma and Mackenzie PN has a greater annual yield (McClelland et al., 2016). PN can be an important source of N, particularly nearshore, whereas DON can be transported further offshore in addition to supporting nearshore production. There is some indication that a low $\delta^{15}N$ of PN in Arctic rivers could be linked to glacial retreat. Nitrogen fixing plants, which are dominant in areas of glacial retreat, impart a characteristically low $\delta^{15}N$ into the terrigenous nitrogen pool (McCLelland et al., 2016 and references therein). While we can surmise that the $\delta^{15}N$ of PN could be imparted onto that of DON or NO_3^- through decomposition or remineralization, because all samples in this study were filtered prior to analysis, we cannot estimate what the $\delta^{15}N$ of PN may be. Future studies would benefit from exploring this source of nitrogen, as PN input is expected to increase with increased riverine discharge and coastal erosion.

Our findings fill important research gaps regarding the greater influence of small rivers in the ECAA on nutrient supply to the Arctic and circulation into the Atlantic. For large terrestrial Arctic rivers, much research has been conducted to weigh the relative influence of factors such as increased nutrient delivery (both organic and inorganic), increased stratification, and changes in light penetration (i.e., due to increased particulate matter input) on primary productivity (Le Fouest et al., 2013; Tank et al., 2012; Terhaar et al., 2021; Thibodeau et al., 2017; Treat et al., 2016; Tremblay et al., 2015). However, our study of smaller Arctic rivers, including those glacially fed, indicates that increased DON delivery may not be a ubiquitous consequence of increased riverine discharge in the Arctic, particularly in the ECAA where these small rivers and tributaries are dominant.

4.2. NO_3^- and DON Cycling in the ECAA and Baffin Bay

Several factors control primary productivity in the Arctic, including nitrogen, iron and light availability (Tremblay et al., 2015). Previous studies suggest that rivers can greatly influence localized nitrogen availability and primary production, though this localized production only represents a relatively minor fraction of net marine primary productivity in the Arctic (Tremblay et al., 2015).

Nitrate concentrations were close to zero in the surface mixed layer at most stations (<10 m depth), though concentration at some surface stations exceeded 1 μmol L^{-1} (Figure 4). This is consistent with N being the limiting nutrient in Arctic regions (Figure 2b). [NO_3^-] increased with depth as expected. The [NO_3^-] found at depth is sourced from the dominant water mass or produced in situ via remineralization. The water in this region is predominantly Pacific-derived (Figure S2 in Supporting Information S1), apart from Eastern Baffin Bay, where the Western Greenland Current brings North Atlantic water to the subsurface. Western Baffin Bay also sees an increase in Atlantic water contribution at depth due to mixing.

Two of the rivers sampled in Western Lancaster Sound (R-DIW, and R-DIW-N) had elevated [NO_3^-] (20 and 47 μmol L^{-1} respectively), which was not reflected in the nearby coastal waters. This suggests the rapid uptake of riverine NO_3^-, or dilution by mixing with the marine end member. This corroborates prior studies wherein riverine supplied NO_3^- is rapidly consumed nearshore (Emmerton et al., 2008; Tremblay et al., 2014, 2015). Discrete chlorophyll-a measurements showed relatively small increases in chlorophyll-a in areas which also had increased NO_3^- (e.g., near Devon Island), and satellite data for July and August 2019 in this region showed higher chlorophyll-a nearshore (Figure S7 in Supporting Information S1). This could indicate localized NO_3^- consumption.

Rivers have been a significant source of bioavailable DON in neighboring coastal waters (Letscher, Hansell, Kadko, & Bates, 2013; Lobbes et al., 2000; Thibodeau et al., 2017). For instance, Lobbes et al. (2000) reported an average [DON] of 12.0 μmol L^{-1} for several Russian rivers, and Thibodeau et al. (2017) measured [DON] ranging

between 13.9 and 21.8 μmol L^{-1} in the Siberian Arctic. Some of these studies found that up to 70% of the terrigenous DON delivered by Arctic rivers was consumed within the shelf waters of the western and Eurasian Arctic (Letscher, Hansell, Kadko, & Bates, 2013; Thibodeau et al., 2017).

DON accumulated to concentrations up to 6.1 μmol L^{-1} in surface waters near Davis Strait (Figure 7a) and could thus sustain primary productivity if a significant fraction of that DON is labile. However, the labile versus recalcitrant DON fractions were not analyzed in this study. DON showed no distinct or consistent trends with depth, and because [NO_3^-] increased rapidly with depth, δ^{15}N–DON was not measured in a significant number of samples beyond the surface mixed layer (Figures S8E–S8H in Supporting Information S1).

Notably, data from this study contrast with findings from other Arctic regions, where [DON] increased with the fraction of river water (Thibodeau et al., 2017) and where terrestrial DON was subsequently consumed in Arctic surface waters (Letscher, Hansell, Kadko, & Bates, 2013; Thibodeau et al., 2017). Instead, [DON] seemed to increase with higher salinity in the mixed surface layer (upper 10 m), though this correlation was overall not significant (Figure 8). This suggests that small but abundant rivers could dilute the marine surface DON pool in the ECAA and Baffin Bay. Deviations from a pure mixing line in Figure 8 suggest that competing sources or transformations are affecting the DON pool, for example, in situ production/consumption by phytoplankton assemblages in the mixed surface waters, inputs from freshwater and buoyancy, or Ekman-driven upwellings (Bhatia et al., 2021; Cape et al., 2019; Thibodeau et al., 2017). The DON pool would also be influenced by the lability of the localized sources. Increased freshwater inputs with low DON concentrations could further stratify the water column in coastal ECAA and Baffin Bay waters, inhibiting vertical exchange with nutrient-rich deep waters, potentially decreasing primary productivity in the region if DIN is concomitantly low.

There was noticeable variation in both DON concentrations and isotopic composition in the surface waters (Figure 7). This could be due to local variations in DON sources. Previous studies have found that the δ^{15}N of DON can reflect the δ^{15}N of the new N source (Knapp et al., 2018). DON produced from a low δ^{15}N source, such as newly nitrified NO_3^- from N_2 fixation, can have a similarly low δ^{15}N−DON. In samples where we were able to measure both δ^{15}N–NO_3^- and DON, the δ^{15}N−DON was on average ∼5‰ lower than that of NO_3^-, with a negative correlation between δ^{15}N−DON and δ^{15}N–NO_3^- (Figure S9 in Supporting Information S1, Pearson R^2 = 0.23, p-value = 0.003). This could indicate DON production from NO_3^-. Knapp et al. (2018) observed a similar trend in the Eastern Tropical South Pacific surface waters, where subsurface DON bracketed the δ^{15}N−NO_3^- by ±3‰. Conversely, the lack of spatial variation in DON isotopic composition and concentration observed in some areas, such as Transect 4, where surface [DON] ranged from 5.7 to 6.1 μmol L^{-1} and δ^{15}N−DON mostly remained constant (4.8–4.9‰), could suggest recalcitrant DON (Bourbonnais et al., 2009; Knapp et al., 2005). This would be in line with observations in the Siberian Arctic where DON in brackish mixing zones was predominantly recalcitrant (Dittmar et al., 2001).

Potential DON consumption was identified only at two main regions in the study area where chlorophyll-a was elevated. We observed a slight negative relationship between chlorophyll-a and DON concentrations in the surface mixed layer in both the northern segment of the Nares Strait and the western half of Transect 1 (Pearson R^2 = 0.75, p-value = 0.04, Spearman $\rho = -1$, p-value = 0.02; Figure 9). This mirrors the relationship between chlorophyll-a and inorganic nutrients in incubation studies (Buapet et al., 2008; Lafarga-De la Cruz et al., 2006), and a similar inverse relationship has been observed between DON and chlorophyll-a in lakes (Berman, 1997). [DON] in the surface mixed layer was also negatively correlated with δ^{15}N (Pearson R^2 = 0.54, p-value = 0.10, Spearman $\rho = -1$, p-value = 0.02, n = 4) (Figure 10) which is indicative of consumption as ^{14}N is preferentially taken up, enriching the remaining DON pool (Knapp et al., 2018). Our isotope effect of 6.9‰, estimated using a closed-system Rayleigh model, is comparable to previously measured isotope effects of DON consumption of 5.5‰ (Knapp et al., 2018). Based on this relationship between [DON] and chlorophyll-a, we posit the occurrence of net DON uptake by phytoplankton, a process which has been proposed in other nearshore Arctic regions (Tank et al., 2012; Thibodeau et al., 2017).

Though Jones Sound also had high chlorophyll, we excluded it in this analysis as we suspect substantial riverine discharge obscured the relationship between chlorophyll-a, DON, and δ^{15}N of DON (Figure S1 in Supporting Information S1). A recalcitrant DON pool could also explain why we did not observe a distinct consumption signal at most stations. Furthermore, any correlation between [DON] and chlorophyll-a is likely hindered by the low spatial resolution of available chlorophyll-a measurements, though satellite data corroborates our

observations of mostly low chlorophyll-a within Baffin Bay (Figure S7 in Supporting Information S1). Furthermore, DON cycling is likely complex and highly dynamic with simultaneous consumption and production decoupled in space and time. These processes could complicate the relationship between chlorophyll-a and DON.

Sea ice melt represents another potential source of DON in the ECAA and Baffin Bay. Similar to surface ice in some glaciers, sea ice can have a higher concentration of DON, as observed in the Antarctic (Fripiat et al., 2014; Dall'Osto et al., 2017). Fripiat et al. (2014) suggested that high DON was released by microbial communities within the sea ice following NO_3^- assimilation. However, no significant correlation was observed between sea ice melt and DON in this study.

5. Conclusions

NO_3^- was the dominant dissolved nitrogen species in the ECAA rivers. We used a steady-state isotopic box model to apportion the sources of NO_3^- in rivers. Our model suggested that NO_3^- assimilation, in addition to mixing between inputs from atmospheric deposition and nitrified NH_4^+, is needed to explain the observed $\delta^{15}N$ and $\delta^{18}O$ of NO_3^- in rivers. NO_3^- putatively derived from the nitrification of permafrost or atmospheric NH_4^+ was found to be a main source of NO_3^- in most rivers, while only a few rivers (e.g., R-ESG) had significant input of NO_3^- from atmospheric deposition. Our stable isotopic data suggest that a significant fraction of this NO_3^- was assimilated in the river and/or rapidly consumed near the shore.

DON concentrations were relatively low in rivers (less than 4.9 μmol L^{-1}). Unlike relationships observed for coastal waters adjacent to major Arctic rivers (Letscher, Hansell, Kadko, & Bates, 2013; Thibodeau et al., 2017; Tremblay et al., 2014), we observed that DON concentrations generally increased with salinity. We posit that increased riverine discharge in the ECAA and Baffin Bay may result in increased stratification of the surface ocean and dilution of the ambient DON pool. However, it is important to note that geochemical signatures of Arctic rivers can vary seasonally (Alkire et al., 2017; Manning et al., 2020), and our river measurements were collected during a relatively narrow period (July 8th–14 August 2019) occurring after the peak annual discharge.

We observed evidence for DON consumption in the northern Nares Strait as well as the western Transect 1. This indicates that DON could be utilized by phytoplankton in the ECAA and Baffin Bay, although the source of this DON as well as its composition and lability require further investigation. We estimated an isotope effect for DON consumption of 6.9‰, which is in line with previous studies (5.5‰; Knapp et al., 2018). Our findings are summarized in Figure 11. This study provides a baseline for DON cycling in the ECAA and Baffin Bay and highlights further areas of research needed to better understand N-cycling in this dynamic region. Due to the high volume of riverine flux from the CAA to the North Atlantic, it is important to better characterize N-cycling within the region and consider the significance and uniqueness of the numerous small rivers and tributaries.

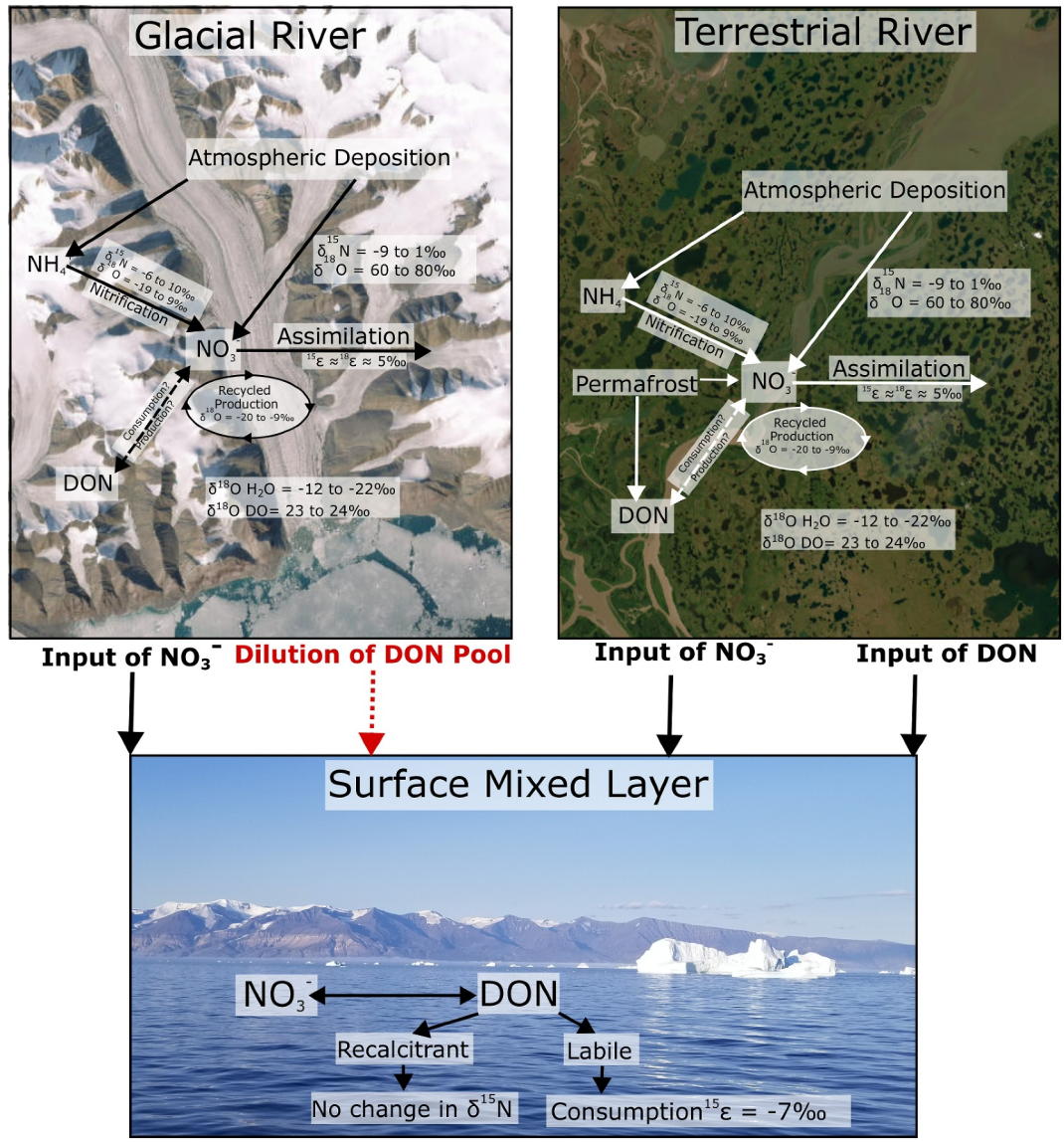

Figure 11. Schematic overview of the processes and findings in the study area. The satellite image of glacial river pictured is of R-ESG, the terrestrial river is the Mackenzie River (Esri, 2023). Surface mixed layer photo was taken off the coast of Greenland during Transect 2.

Data Availability Statement

Data are available at the NSF Arctic Data Center (Bourbonnais & Westbrook, 2023).

Acknowledgments
This work was funded by the National Science Foundation (NSF) (award 1927755 to Bourbonnais). Research on the CCGS Amundsen was funded by ArcticNet, a Network of Centers of Excellence of Canada and the Amundsen Science program, which is supported through Université Laval by the Canada Foundation for Innovation. We also thank Dr. Nadine Lehmann for providing the R code used for Figure 1. Sample collection took place off the shores and within the rivers of Inuit, Inughuit Nunaat, and Kalaallit Nunaat land, and samples were analyzed on Congaree and Tsalaguwetiyi land. We thank the crew of the CCGS Amundsen for making this research possible. We also thank Darcy Perin, Maggie Gaspar, Elise Lumsden, Adrianna Webb, Jaquan High, and Miles Hampton for assistance in sample analysis.

References

Ahmed, M. M. M., Else, B. G. T., Capelle, D., Miller, L. A., & Papakyriakou, T. (2020). Underestimation of surface pCO_2 and air-sea CO_2 fluxes due to freshwater stratification in an Arctic shelf sea, Hudson Bay. *Elementa: Science of the Anthropocene*, *8*(1). https://doi.org/10.1525/elementa.084

Alkire, M. B., Falkner, K. K., Boyd, T., & Macdonald, R. W. (2010). Sea ice melt and meteoric water distributions in Nares Strait, Baffin Bay, and the Canadian Arctic Archipelago. *Journal of Marine Research*, *68*(6), 767–798. https://doi.org/10.1357/002224010796673867

Alkire, M. B., Jacobson, A. D., Lehn, G. O., Macdonald, R. W., & Rossi, M. W. (2017). On the geochemical heterogeneity of rivers draining into the straits and channels of the Canadian Arctic Archipelago. *Journal of Geophysical Research: Biogeosciences*, *122*(10), 2527–2547. https://doi.org/10.1002/2016jg003723

Altieri, K. E., Fawcett, S. E., Peters, A. J., Sigman, D. M., & Hastings, M. G. (2016). Marine biogenic source of atmospheric organic nitrogen in the subtropical North Atlantic. *Proceedings of the National Academy of Sciences of the United States of America*, *113*(4), 925–930. https://doi.org/10.1073/pnas.1516847113

Alves, R. J. E., Wanek, W., Zappe, A., Richter, A., Svenning, M. M., Schleper, C., & Urich, T. (2013). Nitrification rates in Arctic soils are associated with functionally distinct populations of ammonia-oxidizing archaea. *The ISME Journal*, *7*(8), 1620–1631. https://doi.org/10.1038/ismej.2013.35

Ansari, A. H., Hodson, A. J., Heaton, T. H. E., Kaiser, J., & Marca-Bell, A. (2013). Stable isotopic evidence for nitrification and denitrification in a High Arctic glacial ecosystem. *Biogeochemistry*, *113*(1–3), 341–357. https://doi.org/10.1007/s10533-012-9761-9

Arendt, C. A., Heikoop, J. M., Newman, B. D., Wilson, C. J., Graham, D. E., Dafflon, B., et al. (2016). Isotopic and chemical identification of hydrological pathways in a watershed underlain by shallow discontinuous permafrost. In *Conference Presentation Abstract*. American Geophysical Union Fall Meeting.

Arrigo, K., & van Dijken, G. L. (2015). Continued increases in Arctic Ocean primary production. *Progress in Oceanography*, *136*, 60–70. https://doi.org/10.1016/j.pocean.2015.05.002

Beaton, A. D., Wadham, J. L., Hawkings, J., Bagshaw, E. A., Lamarche-Gagnon, G., Mowlem, M. C., & Tranter, M. (2017). High-Resolution in situ measurement of nitrate in runoff from the Greenland Ice Sheet. *Environmental Science and Technology*, *51*(21), 12518–12527. https://doi.org/10.1021/acs.est.7b03121

Berman, T. (1997). Dissolved organic nitrogen utilization by an Aphanizomenon bloom in Lake Kinneret. *Journal of Plankton Research*, *19*(5), 577–586. https://doi.org/10.1093/plankt/19.5.577

Bhatia, M. P., Waterman, S., Burgess, D. O., Williams, P. L., Bundy, R. M., Mellett, T., et al. (2021). Glaciers and nutrients in the Canadian Arctic Archipelago marine system. *Global Biogeochemical Cycles*, *35*(8). https://doi.org/10.1029/2021GB006976

Bif, M. B., Bourbonnais, A., Hansell, D. A., Granger, J., Westbrook, H. C., & Altabet, M. A. (2022). Controls on surface distributions of dissolved organic carbon and nitrogen in the southeast Pacific Ocean. *Marine Chemistry*, *244*, 104136. https://doi.org/10.1016/j.marchem.2022.104136

Bintanja, R., & Selten, F. M. (2014). Future increases in Arctic precipitation linked to local evaporation and sea-ice retreat. *Nature*, *509*(7501), 479–482. https://doi.org/10.1038/nature13259

Boshers, D. S., Granger, J., Tobias, C. R., Böhlke, J. K., & Smith, R. L. (2019). Constraining the oxygen isotopic composition of nitrate produced by nitrification. *Environmental Science and Technology*, *53*(3), 1206–1216. https://doi.org/10.1021/acs.est.8b03386

Bourbonnais, A., Lehmann, M. F., Waniek, J. J., & Schulz-Bull, D. E. (2009). Nitrate isotope anomalies reflect N_2 fixation in the Azores Front region (subtropical NE Atlantic). *Journal of Geophysical Research*, *114*(C3). https://doi.org/10.1029/2007jc004617

Bourbonnais, A., & Westbrook, H. C. (2023). Dissolved nitrogen concentrations and stable isotopic composition in the eastern Canadian Arctic Archipelago and Baffin Bay, Legs 2a and 2b of the ArcticNet expedition, CCGS Amundsen, July 5th to August 15th 2019 [Dataset]. *Arctic Data Center*. https://doi.org/10.18739/A2JM23H6Z

Braman, R. S., & Hendrix, S. A. (1989). Nanogram nitrite and nitrate determination in environmental and biological materials by Vanadium(III) reduction with chemiluminescence detection. *Analytical Chemistry*, *61*(24), 2715–2718. https://doi.org/10.1021/ac00199a007

Bronk, D. A., Glibert, P., Malone, T., Banahan, S., & Sahlsten, E. (1998). Inorganic and organic nitrogen cycling in Chesapeake Bay: Autotrophic versus heterotrophic processes and relationships to carbon flux. *Aquatic Microbial Ecology*, *15*, 177–189. https://doi.org/10.3354/ame015177

Bronk, D. A., See, J. H., Bradley, P., & Killberg, L. (2007). DON as a source of bioavailable nitrogen for phytoplankton. *Biogeosciences*, *4*(3), 283–296. https://doi.org/10.5194/bg-4-283-2007

Brown, K. A., Manning, C. C. M., Jones, S. F., Izett, R. W., Capelle, D. W., Else, B. G. T., et al. (2022). *Canadian Arctic Archipelago rivers program: Nutrient, dissolved organic carbon, and water isotope data 2016–2019*. PANGAEA. https://doi.org/10.1594/PANGAEA.945702

Buapet, P., Hiranpan, R., Ritchie, R. J., & Prathep, A. (2008). Effect of nutrient inputs on growth, chlorophyll, and tissue nutrient concentration of *Ulva reticulata* from a tropical habitat. *ScienceAsia*, *34*(2), 245. https://doi.org/10.2306/scienceasia1513-1874.2008.34.245

Buchwald, C., Santoro, A. E., McIlvin, M. R., & Casciotti, K. L. (2012). Oxygen isotopic composition of nitrate and nitrite produced by nitrifying cocultures and natural marine assemblages. *Limnology & Oceanography*, *57*(5), 1361–1375. https://doi.org/10.4319/lo.2012.57.5.1361

Burt, W. J., Westberry, T. K., Behrenfeld, M. J., Zeng, C., Izett, R. W., & Tortell, P. D. (2018). Carbon: Chlorophyll ratios and net primary productivity of subarctic Pacific surface waters derived from autonomous shipboard sensors. *Global Biogeochemical Cycles*, *32*(2), 267–288. https://doi.org/10.1002/2017gb005783

Cape, M. R., Straneo, F., Beaird, N., Bundy, R. M., & Charette, M. A. (2019). Nutrient release to oceans from buoyancy-driven upwelling at Greenland tidewater glaciers. *Nature Geoscience*, *12*(1), 34–39. https://doi.org/10.1038/s41561-018-0268-4

Carpenter, E. J., Harvey, H. R., Fry, B., & Capone, D. G. (1997). Biogeochemical tracers of the marine cyanobacterium *Trichodesmium*. *Deep Sea Research Part I: Oceanographic Research Papers*, *44*(1), 27–38. https://doi.org/10.1016/S0967-0637(96)00091-X

Casciotti, K. L., McIlvin, M., & Buchwald, C. (2010). Oxygen isotopic exchange and fractionation during bacterial ammonia oxidation. *Limnology & Oceanography*, *55*(2), 753–762. https://doi.org/10.4319/lo.2010.55.2.0753

Casciotti, K. L., Sigman, D. M., Hastings, M. G., Böhlke, J. K., & Hilkert, A. (2002). Measurement of the oxygen isotopic composition of nitrate in seawater and freshwater using the denitrifier method. *Analytical Chemistry*, *74*(19), 4905–4912. https://doi.org/10.1021/ac020113w

Clark, S. C., Granger, J., Mastorakis, A., Aguilar-Islas, A., & Hastings, M. G. (2020). An investigation into the origin of nitrate in Arctic Sea Ice. *Global Biogeochemical Cycles*, *34*(2). https://doi.org/10.1029/2019gb006279

Dall'Osto, M., Ovadnevaite, J., Paglione, M., Beddows, D. C. S., Ceburnis, D., Cree, C., et al. (2017). Antarctic sea ice region as a source of biogenic organic nitrogen in aerosols. *Scientific Reports*, *7*(1), 6047. https://doi.org/10.1038/s41598-017-06188-x

Dalsgaard, T., Stewart, F. J., Thamdrup, B., Brabandere, L. D., Revsbech, N. P., Ulloa, O., et al. (2014). Oxygen at nanomolar levels reversibly suppresses process rates and gene expression in anammox and denitrification in the oxygen minimum zone off northern Chile. *mBio*, *5*(6). https://doi.org/10.1128/mbio.01966-14

Dittmar, T., Fitznar, H. P., & Kattner, G. (2001). Origin and biogeochemical cycling of organic nitrogen in the eastern Arctic Ocean as evident from D- and L-amino acids. *Geochimica et Cosmochimica Acta*, *65*(22), 4103–4114. https://doi.org/10.1016/s0016-7037(01)00688-3

Emmerton, C. A., Lesack, L. F. W., & Vincent, W. F. (2008). Nutrient and organic matter patterns across the Mackenzie River, estuary and shelf during the seasonal recession of sea-ice. *Journal of Marine Systems*, *74*(3–4), 741–755. https://doi.org/10.1016/j.jmarsys.2007.10.001

Esri. (2023). World imagery basemap [Software]. *Esri and Maxar*. Retrieved from https://www.arcgis.com/home/item.html?id=10df2279f9684e4a9f6a7f08febac2a9

Fawcett, S. E., Lomas, M. W., Casey, J. R., Ward, B. B., & Sigman, D. M. (2011). Assimilation of upwelled nitrate by small eukaryotes in the Sargasso Sea. *Nature Geoscience*, *4*(10), 717–722. https://doi.org/10.1038/ngeo1265

Feng, D., Gleason, C. J., Lin, P., Yang, X., Pan, M., & Ishitsuka, Y. (2021). Recent changes to Arctic river discharge. *Nature Communications*, *12*(1), 6917. https://doi.org/10.1038/s41467-021-27228-1

Fouché, J., Christiansen, C. T., Lafrenière, M. J., Grogan, P., & Lamoureux, S. F. (2020). Canadian permafrost stores large pools of ammonium and optically distinct dissolved organic matter. *Nature Communications*, *11*(1), 4500. https://doi.org/10.1038/s41467-020-18331-w

Francis, A., Ganeshram, R. S., Tuerena, R. E., Spencer, R. G. M., Holmes, R. M., Rogers, J. A., & Mahaffey, C. (2023). Permafrost degradation and nitrogen cycling in Arctic Rivers: Insights from stable nitrogen isotope studies. *Biogeosciences*, *20*(2), 365–382. https://doi.org/10.5194/bg-20-365-2023

Frey, K. E., & McClelland, J. W. (2009). Impacts of permafrost degradation on Arctic River biogeochemistry. *Hydrological Processes*, *23*(1), 169–182. https://doi.org/10.1002/hyp.7196

Frey, K. E., McClelland, J. W., Holmes, R. M., & Smith, L. C. (2007). Impacts of climate warming and permafrost thaw on the riverine transport of nitrogen and phosphorus to the Kara Sea. *Journal of Geophysical Research*, *112*(G4), 112. https://doi.org/10.1029/2006jg000369

Fripiat, F., Sigman, D. M., Fawcett, S. E., Rafter, P. A., Weigand, M. A., & Tison, J. L. (2014). New insights into sea ice nitrogen biogeochemical dynamics from the nitrogen isotopes. *Global Biogeochemical Cycles*, *28*(2), 115–130. https://doi.org/10.1002/2013gb004729

Fuhrman, J. (1987). Close coupling between release and uptake of dissolved free amino acids in seawater studied by an isotope dilution approach. *Marine Ecology Progress Series*, *37*(1), 45–52. https://doi.org/10.3354/meps037045

Granger, J., & Sigman, D. M. (2009). Removal of nitrite with sulfamic acid for nitrate N and O isotope analysis with the denitrifier method. *Rapid Communications in Mass Spectrometry*, *23*(23), 3753–3762. https://doi.org/10.1002/rcm.4307

Granger, J., Sigman, D. M., Gagnon, J., Tremblay, J., & Mucci, A. (2018). On the properties of the Arctic halocline and deep water masses of the Canada Basin from nitrate isotope ratios. *Journal of Geophysical Research: Oceans*, *123*(8), 5443–5458. https://doi.org/10.1029/2018jc014110

Granger, J., Sigman, D. M., Lehmann, M. F., & Tortell, P. D. (2008). Nitrogen and oxygen isotope fractionation during dissimilatory nitrate reduction by denitrifying bacteria. *Limnology & Oceanography*, *53*(6), 2533–2545. https://doi.org/10.4319/lo.2008.53.6.2533

Granger, J., Sigman, D. M., Needoba, J. A., & Harrison, P. J. (2004). Coupled nitrogen and oxygen isotope fractionation of nitrate during assimilation by cultures of marine phytoplankton. *Limnology & Oceanography*, *49*(5), 1763–1773. https://doi.org/10.4319/lo.2004.49.5.1763

Haine, T. W. N., Cury, B., Gerdes, R., Hansen, E., Karcher, M., Lee, C., et al. (2015). Arctic freshwater export: Status, mechanisms, and prospects. *Global and Planetary Change*, *124*, 13–35. https://doi.org/10.1016/j.gloplacha.2014.11.013

Hastings, M. G., Sigman, D. M., & Lipschultz, F. (2003). Isotopic evidence for source changes of nitrate in rain at Bermuda. *Journal of Geophysical Research*, *108*(D24). https://doi.org/10.1029/2003jd003789

Hastings, M. G., Steig, E. J., & Sigman, D. M. (2004). Seasonal variations in N and O isotopes of nitrate in snow at Summit, Greenland: Implications for the study of nitrate in snow and ice cores. *Journal of Geophysical Research*, *109*(D20), 109. https://doi.org/10.1029/2004jd004991

Heikoop, J. M., Throckmorton, H. M., Newman, B. D., Perkins, G. B., Iversen, C. M., Chowdhury, T. R., et al. (2015). Isotopic identification of soil and permafrost nitrate sources in an Arctic tundra ecosystem. *Journal of Geophysical Research: Biogeosciences*, *120*(6), 1000–1017. https://doi.org/10.1002/2014jg002883

Holland, A. T., Williamson, C. J., Sgouridis, F., Tedstone, A. J., McCutcheon, J., Cook, J. M., et al. (2019). Dissolved organic nutrients dominate melting surface ice of the Dark Zone (Greenland Ice Sheet). *Biogeosciences*, *16*(16), 3283–3296. https://doi.org/10.5194/bg-16-3283-2019

Holmes, R. M., McClelland, J. W., Peterson, B. J., Tank, S. E., Bulygina, E., Eglinton, T. I., et al. (2012). Seasonal and annual fluxes of nutrients and organic matter from large rivers to the Arctic Ocean and surrounding seas. *Estuaries and Coasts*, *35*(2), 369–382. https://doi.org/10.1007/s12237-011-9386-6

Johnston, J. C., & Thiemens, M. H. (1997). The isotopic composition of tropospheric ozone in three environments. *Journal of Geophysical Research*, *102*(D21), 25395–25404. https://doi.org/10.1029/97jd02075

Juranek, L. W. (2022). Changing biogeochemistry of the Arctic Ocean: Surface nutrient and CO_2 cycling in a warming, melting north. *Oceanography*, *35*(3–4), 144–155. https://doi.org/10.5670/oceanog.2022.120

Kaiser, K., Canedo-Oropeza, M., McMahon, R., & Amon, R. M. W. (2017). Origins and transformations of dissolved organic matter in large Arctic Rivers. *Scientific Reports*, *7*(1), 13064. https://doi.org/10.1038/s41598-017-12729-1

Kiddon, J., Bender, M. L., Orchardo, J., Caron, D. A., Goldman, J. C., & Dennett, M. (1993). Isotopic fractionation of oxygen by respiring marine organisms. *Global Biogeochemical Cycles*, *7*(3), 679–694. https://doi.org/10.1029/93gb01444

Knapp, A. N., Casciotti, K. L., & Prokopenko, M. G. (2018). Dissolved organic nitrogen production and consumption in Eastern tropical South Pacific surface waters. *Global Biogeochemical Cycles*, *32*(5), 769–783. https://doi.org/10.1029/2017gb005875

Knapp, A. N., Sigman, D. M., & Lipschultz, F. (2005). N isotopic composition of dissolved organic nitrogen and nitrate at the Bermuda Atlantic time-series study site. *Global Biogeochemical Cycles*, *19*(1). https://doi.org/10.1029/2004gb002320

Krankowsky, D., Bartecki, F., Klees, G. G., Mauersberger, K., Schellenbach, K., & Stehr, J. (1995). Measurement of heavy isotope enrichment in tropospheric ozone. *Geophysical Research Letters*, *22*(13), 1713–1716. https://doi.org/10.1029/95gl01436

Lafarga-De la Cruz, F., Valenzuela-Espinoza, E., Millán-Núñez, R., Trees, C. C., Santamaría-del-Ángel, E., & Núñez-Cebrero, F. (2006). Nutrient uptake, chlorophyll-a and carbon fixation by *Rhodomonas* sp. (Cryptophyceae) cultured at different irradiance and nutrient concentrations. *Aquacultural Engineering*, *35*(1), 51–60. https://doi.org/10.1016/j.aquaeng.2005.08.004

Le Fouest, V., Babin, M., & Tremblay, J.-É. (2013). The fate of riverine nutrients on Arctic shelves. *Biogeosciences*, *10*(6), 3661–3677. https://doi.org/10.5194/bg-10-3661-2013

Lehmann, N., Kienast, M., Granger, J., Bourbonnais, A., Altabet, M. A., & Tremblay, J.-É. (2019). Remote western Arctic nutrients fuel remineralization in deep Baffin Bay. *Global Biogeochemical Cycles*, *33*(6), 649–667. https://doi.org/10.1029/2018gb006134

Lehmann, N., Kienast, M., Granger, J., & Tremblay, J.-É. (2022). Physical and biogeochemical influences on nutrients through the Canadian Arctic Archipelago: Insights from nitrate isotope ratios. *Journal of Geophysical Research: Oceans*, *127*(3). https://doi.org/10.1029/2021jc018179

Letscher, R. T., Hansell, D. A., Carlson, C. A., Lumpkin, R., & Knapp, A. N. (2013). Dissolved organic nitrogen in the global surface ocean: Distribution and fate. *Global Biogeochemical Cycles*, *27*(1), 141–153. https://doi.org/10.1029/2012gb004449

Letscher, R. T., Hansell, D. A., Kadko, D., & Bates, N. R. (2013). Dissolved organic nitrogen dynamics in the Arctic Ocean. *Marine Chemistry*, *148*, 1–9. https://doi.org/10.1016/j.marchem.2012.10.002

Lewis, K. M., van Dijken, G. L., & Arrigo, K. R. (2020). Changes in phytoplankton concentration now drive increased Arctic Ocean primary production. *Science*, *369*(6500), 198–202. https://doi.org/10.1126/science.aay8380

Link, P. M., & Tol, R. S. J. (2009). Economic impacts on key Barents Sea fisheries arising from changes in the strength of the Atlantic thermohaline circulation. *Global Environmental Change*, *19*(4), 422–433. https://doi.org/10.1016/j.gloenvcha.2009.07.007

Lobbes, J. M., Fitznar, H. P., & Kattner, G. (2000). Biogeochemical characteristics of dissolved and particulate organic matter in Russian rivers entering the Arctic Ocean. *Geochimica et Cosmochimica Acta*, *26*(17), 2973–2983. https://doi.org/10.1016/s0016-7037(00)00409-9

Louiseize, N. L., Lafrenière, M. J., & Hastings, M. G. (2014). Stable isotopic evidence of enhanced export of microbially derived NO_3^- following active layer slope disturbance in the Canadian High Arctic. *Biogeochemistry*, *121*(3), 565–580. https://doi.org/10.1007/s10533-014-0023-x

Manning, C. C. M., Preston, V. L., Jones, S. F., Michel, A. P. M., Nicholson, D. P., Duke, P. J., et al. (2020). River inflow dominates methane emissions in an Arctic coastal system. *Geophysical Research Letters*, *47*(10). https://doi.org/10.1029/2020gl087669

McClelland, J. W., Holmes, R. M., Peterson, B. J., Raymond, P. A., Striegl, R. G., Zhulidov, A. V., et al. (2016). Particulate organic carbon and nitrogen export from major Arctic rivers. *Global Biogeochemical Cycles*, *30*(5), 629–643. https://doi.org/10.1002/2015gb005351

McLaughlin, F. A., & Carmack, E. C. (2010). Deepening of the nutricline and chlorophyll maximum in the Canada Basin interior, 2003–2009. *Geophysical Research Letters*, *37*(24). https://doi.org/10.1029/2010gl045459

Minagawa, M., & Wada, E. (1986). Nitrogen isotope ratios of red tide organisms in the East China Sea: A characterization of biological nitrogen fixation. *Marine Chemistry*, *19*(3), 245–259. https://doi.org/10.1016/0304-4203(86)90026-5

Moschonas, G., Gowen, R. J., Paterson, R. F., Mitchell, E., Stewart, B. M., McNeill, S., et al. (2017). Nitrogen dynamics and phytoplankton community structure: The role of organic nutrients. *Biogeochemistry*, *134*(1), 125–145. https://doi.org/10.1007/s10533-017-0351-8

O'Donnell, J. A., Aiken, G. R., Swanson, D. K., Panda, S., Butler, K. D., & Baltensperger, A. P. (2016). Dissolved organic matter composition of Arctic rivers: Linking permafrost and parent material to riverine carbon. *Global Biogeochemical Cycles*, *30*(12), 1811–1826. https://doi.org/10.1002/2016GB005482

Peterson, B. J., Holmes, R. M., McClelland, J. W., Vörösmarty, C. J., Lammers, R. B., Shiklomanov, A. I., et al. (2002). Increasing river discharge to the Arctic Ocean. *Science*, *298*(5601), 2171–2173. https://doi.org/10.1126/science.1077445

Rafter, P. A., DiFiore, P. J., & Sigman, D. M. (2013). Coupled nitrate nitrogen and oxygen isotopes and organic matter remineralization in the Southern and Pacific Oceans. *Journal of Geophysical Research: Oceans*, *118*(10), 4781–4794. https://doi.org/10.1002/jgrc.20316

Rafter, P. A., & Sigman, D. M. (2016). Spatial distribution and temporal variation of nitrate nitrogen and oxygen isotopes in the upper equatorial Pacific Ocean. *Limnology & Oceanography*, *61*(1), 14–31. https://doi.org/10.1002/lno.10152

Rogalla, B., Allen, S. E., Colombo, M., Myers, P. G., & Orians, K. J. (2023). Continental and glacial runoff fingerprints in the Canadian Arctic Archipelago, the Inuit Nunangat Ocean. *Journal of Geophysical Research: Biogeosciences*, *128*(5). https://doi.org/10.1029/2022JG007072

Rood, S. B., Kaluthota, S., Philipsen, L. J., Rood, N. J., & Zanewich, K. P. (2017). Increasing discharge from the Mackenzie River system to the Arctic Ocean. *Hydrological Processes*, *31*(1), 150–160. https://doi.org/10.1002/hyp.10986

Sanders, T., Fiencke, C., Fuchs, M., Haugk, C., Juhls, B., Mollenhauer, G., et al. (2022). Seasonal nitrogen fluxes of the Lena River Delta. *Ambio*, *51*(2), 423–438. https://doi.org/10.1007/s13280-021-01665-0

Schlitzer, R. (2021). Ocean data viewer [Software]. Retrieved from https://odv.awi.de

Sigman, D. M., Casciotti, K. L., Andreani, M., Barford, C., Galanter, M. B. J. K., & Böhlke, J. K. (2001). A bacterial method for the nitrogen isotopic analysis of nitrate in seawater and freshwater. *Analytical Chemistry*, *73*(17), 4145–4153. https://doi.org/10.1021/ac010088e

Sipler, R., & Bronk, D. A. (2014). Dynamics of dissolved organic nitrogen. In D. A. Hansel & C. A. Carlson (Eds.), *Biogeochemistry of dissolved organic matter* (2nd ed., pp. 127–232). https://doi.org/10.1016/b978-0-12-405940-5.00004-2

Snyder, L., & Bowden, W. B. (2014). Nutrient dynamics in an oligotrophic Arctic stream monitored in situ by wet chemistry methods. *Water Resources Research*, *50*(3), 2039–2049. https://doi.org/10.1002/2013wr014317

Speetjens, N. J., Hugelius, G., Gumbricht, T., Lantuit, H., Berghuijs, W. R., Pika, P. A., et al. (2023). The pan-Arctic catchment database (ARCADE). *Earth System Science Data*, *15*(2), 541–554. https://doi.org/10.5194/essd-15-541-2023

Tang, C. C. L., Ross, C. K., Yao, T., Petrie, B., DeTracey, B. M., & Dunlap, E. (2004). The circulation, water masses and sea-ice of Baffin Bay. *Progress in Oceanography*, *63*(4), 183–228. https://doi.org/10.1016/j.pocean.2004.09.005

Tank, S. E., Manizza, M., Holmes, R. M., McClelland, J. W., & Peterson, B. J. (2012). The processing and impact of dissolved riverine nitrogen in the Arctic Ocean. *Estuaries and Coasts*, *35*(2), 401–415. https://doi.org/10.1007/s12237-011-9417-3

Telling, J., Stibal, M., Anesio, A. M., Tranter, M., Nias, I., Cook, J., et al. (2012). Microbial nitrogen cycling on the Greenland Ice Sheet. *Biogeosciences*, *9*(7), 2431–2442. https://doi.org/10.5194/bg-9-2431-2012

Terhaar, J., Lauerwald, R., Regnier, P., Gruber, N., & Bopp, L. (2021). Around one third of current Arctic Ocean primary production sustained by rivers and coastal erosion. *Nature Communications*, *12*(1), 169. https://doi.org/10.1038/s41467-020-20470-z

Thibodeau, B., Bauch, D., & Voss, M. (2017). Nitrogen dynamic in Eurasian coastal Arctic ecosystem: Insight from nitrogen isotope. *Global Biogeochemical Cycles*, *31*(5), 836–849. https://doi.org/10.1002/2016gb005593

Treat, C. C., Wollheim, W. M., Varner, R. K., & Bowden, W. B. (2016). Longer thaw seasons increase nitrogen availability for leaching during fall in tundra soils. *Environmental Research Letters*, *11*(6), 064013. https://doi.org/10.1088/1748-9326/11/6/064013

Tremblay, J.-É., Anderson, L. G., Matrai, P., Coupel, P., Bélanger, S., Michel, C., & Reigstad, M. (2015). Global and regional drivers of nutrient supply, primary production and CO_2 drawdown in the changing Arctic Ocean. *Progress in Oceanography*, *139*, 171–196. https://doi.org/10.1016/j.pocean.2015.08.009

Tremblay, J.-É., Michel, C., Hobson, K. A., Gosselin, M., & Price, N. M. (2006). Bloom dynamics in early opening waters of the Arctic Ocean. *Limnology & Oceanography*, *51*(2), 900–912. https://doi.org/10.4319/lo.2006.51.2.0900

Tremblay, J.-É., Raimbault, P., Garcia, N., Lansard, B., Babin, M., & Gagnon, J. (2014). Impact of river discharge, upwelling and vertical mixing on the nutrient loading and productivity of the Canadian Beaufort Shelf. *Biogeosciences*, *11*(17), 4853–4868. https://doi.org/10.5194/bg-11-4853-2014

Vonk, J. E., Tank, S. E., Bowden, W. B., Laurion, I., Vincent, W. F., Alekseychik, P., et al. (2015). Reviews and syntheses: Effects of permafrost thaw on Arctic aquatic ecosystems. *Biogeosciences*, *12*(23), 7129–7167. https://doi.org/10.5194/bg-12-7129-2015

Wadham, J. L., Hawkings, J., Telling, J., Chandler, D., Alcock, J., O'Donnell, E., et al. (2016). Sources, cycling and export of nitrogen on the Greenland Ice Sheet. *Biogeosciences*, *13*(22), 6339–6352. https://doi.org/10.5194/bg-13-6339-2016

Wagner, D., Spieck, E., Bock, E., & Pfeiffer, E.-M. (2002). Microbial life in terrestrial permafrost: Methanogenesis and nitrification in gelisols as potentials for exobiological process. In G. Horneck & C. Baumstark-Khan (Eds.), *Astrobiology* (pp. 143–159). https://doi.org/10.1007/978-3-642-59381-9_10

Wang, X., & Veizer, J. (2000). Respiration–photosynthesis balance of terrestrial aquatic ecosystems, Ottawa area, Canada. *Geochimica et Cosmochimica Acta*, *64*(22), 3775–3786. https://doi.org/10.1016/s0016-7037(00)00477-4

Wassmann, P., Duarte, C. M., Agusti, S., & Sejr, M. K. (2011). Footprints of climate change in the Arctic marine ecosystem. *Global Change Biology*, *17*(2), 1235–1249. https://doi.org/10.1111/j.1365-2486.2010.02311.x

Weigand, M. A., Foriel, J., Barnett, B., Oleynik, S., & Sigman, D. M. (2016). Updates to instrumentation and protocols for isotopic analysis of nitrate by the denitrifier method. *Rapid Communications in Mass Spectrometry*, *30*(12), 1365–1383. https://doi.org/10.1002/rcm.7570

Whalen, S. C., & Cornwell, J. C. (1985). Nitrogen, phosphorus, and organic carbon cycling in an Arctic Lake. *Canadian Journal of Fisheries and Aquatic Sciences*, *42*(4), 797–808. https://doi.org/10.1139/f85-102

Wu, P., Wood, R., & Stott, P. (2005). Human influence on increasing Arctic river discharges. *Geophysical Research Letters*, *32*(2). https://doi.org/10.1029/2004gl021570

Wynn, P. M., Hodson, A. J., Heaton, T. H. E., & Chenery, S. R. (2007). Nitrate production beneath a high Arctic glacier, Svalbard. *Chemical Geology*, *244*(1–2), 88–102. https://doi.org/10.1016/j.chemgeo.2007.06.008

Yamamoto-Kawai, M., Carmack, E., & McLaughlin, F. (2006). Nitrogen balance and Arctic throughflow. *Nature*, *443*(7107), 43. https://doi.org/10.1038/443043a

Ye, F., Guo, W., Wei, G., & Jia, G. (2018). The sources and transformations of dissolved organic matter in the Pearl River Estuary, China, as revealed by stable isotopes. *Journal of Geophysical Research: Oceans*, *123*(9), 6893–6908. https://doi.org/10.1029/2018jc014004